



UNIVERSITY OF LEEDS

This is a repository copy of *Contribution of RC columns and masonry wall to the shear resistance of masonry infilled RC frames containing different in size window and door openings*.

White Rose Research Online URL for this paper:
<http://eprints.whiterose.ac.uk/144559/>

Version: Accepted Version

Article:

Penava, D, Sarhosis, V orcid.org/0000-0002-8604-8659, Kožar, I et al. (1 more author) (2018) Contribution of RC columns and masonry wall to the shear resistance of masonry infilled RC frames containing different in size window and door openings. *Engineering Structures*, 172. pp. 105-130. ISSN 0141-0296

<https://doi.org/10.1016/j.engstruct.2018.06.007>

(c) 2018, Elsevier Ltd. This manuscript version is made available under the CC BY-NC-ND 4.0 license <https://creativecommons.org/licenses/by-nc-nd/4.0/>

Reuse

This article is distributed under the terms of the Creative Commons Attribution-NonCommercial-NoDerivs (CC BY-NC-ND) licence. This licence only allows you to download this work and share it with others as long as you credit the authors, but you can't change the article in any way or use it commercially. More information and the full terms of the licence here: <https://creativecommons.org/licenses/>

Takedown

If you consider content in White Rose Research Online to be in breach of UK law, please notify us by emailing eprints@whiterose.ac.uk including the URL of the record and the reason for the withdrawal request.



eprints@whiterose.ac.uk
<https://eprints.whiterose.ac.uk/>

Contribution of RC columns and masonry wall to the shear resistance of masonry infilled RC frames containing different in size window and door openings

Davorin Penava^{a*}, Vasilis Sarhosis^b, Ivica Kožar^c, Ivica Guljaš^d

^a*Faculty of Civil Engineering Osijek, Josip Juraj Strossmayer University of Osijek, Osijek, Croatia, dpenava@gfos.hr*

^b*School of Civil Engineering and Geosciences, Newcastle University, Newcastle Upon Tyne, NE1 7RU, UK,*

Vasilis.Sarhosis@newcastle.ac.uk

^c*Faculty of Civil Engineering, University of Rijeka, Rijeka, Croatia, ivica.kozar@uniri.hr*

^d*Faculty of Civil Engineering Osijek, Josip Juraj Strossmayer University of Osijek, Osijek, Croatia, iguljas@gfos.hr*

Abstract

In design, the contribution of the masonry infill wall to the shear resistance of the infilled frame structural system is often neglected. However, past research shows that ignoring this element can lead to inaccurate predictions of the system's behaviour. This paper investigates the influence of the opening type, size and position on the shear resistance and deformation capacity of individual components (infill and frame) in masonry infilled reinforced concrete (RC) frame structures. A computational model based on the non-linear finite element (FE) method of analysis has been developed. The computational model has been validated against a series of experimental tests carried out in the laboratory. An extensive parametric study was carried out and the influence of differences in size and location of window and door openings on the shear resistance of infilled frame was investigated. As a measure of the influence of the infill component, a shear resistance ratio for the frame was introduced. The normalized shear resistance capacity ratio represented the ratio of the shear force taken by the frame component (infilled frame case) divided by the shear force induced by the RC bare frame at observed drift ratios (damage grades). From the results analysis, it was found that the type of opening influences the design characteristics of the infilled RC frame. In particular, the shear resistance at columns of the infilled RC frame with a window opening is lower than the shear resistance of the columns of the RC frame. In contrast, the shear resistance at the columns of the infilled RC frame with a door opening is higher than the shear resistance of the columns of the RC frame, and in this case the contribution of the shear capacity of the frame is underestimated.

Keywords

Shear resistance, deformation capacity, reinforced concrete frame with masonry infill walls, opening, computational analysis, structural component contribution

***Corresponding author:** Davorin Penava, *Faculty of Civil Engineering Osijek, Josip Juraj Strossmayer University of Osijek, Osijek, Croatia, dpenava@gfos.hr*

1 Introduction

Structural frames, using reinforced concrete (RC), are commonly used in the construction of multi-storey buildings. RC frames are infilled by masonry walls (with and without openings), which are not only used for architectural purposes (i.e., to separate the internal spaces from the external environment) but also for providing complimentary in-plane shear resistance to the structure. During an earthquake, masonry infill walls influence the resistance of the structure and can undergo premature failure in the in-plane and out-of-plane directions. However, in design, it is common practice to neglect the stiffness contribution of the masonry infill wall, which can lead to inaccurate predictions of the stiffness, strength and ductility of the structure. Therefore, in design calculations, the omission of the contribution of masonry infill walls may result in significant underestimation of the overall design capacity of the structure. There has been extensive experimental and computational research work carried out over the last six decades; however, there is still a lack of understanding of the interaction between the frame and infill walls in RC structures. This is partly attributed to incomplete knowledge of the “composite” behaviour of the frame and the infill wall, as well as due to the lack of conclusive experimental and analytical results to substantiate a reliable design procedure for this type of structure (Liu et al. 2011; Moghadam et al. 2006; Liauw & Kwan 1985; Riddington & Smith 1977).

In 1956, Polyakov was the first to experimentally study the behaviour of masonry infilled frames subjected to lateral loads. Full-scale experimental tests were carried out, and the effect of masonry units, mortar strength and loading type applied to the structure were investigated. From this experimental campaign, it was highlighted that, at low levels of lateral load, the infill wall behaves as a monolithic structure. However, as the lateral load increases, step-wise cracks along the diagonal compression of the infill wall were observed. Therefore, Polyakov suggested that masonry infilled frames can be analysed as equivalent braced frames with a compression diagonal strut replacing the infill wall. Later, in 1958, Benjamin and Williams, using typical specimens of US construction, found that, upon increased lateral loading, the masonry infill wall can separate from the RC frame. In this situation, the only points of contact are the loaded corner and the diagonally opposite corner of the frame. Later, several experimental investigations on the lateral stiffness and strength of masonry infilled frames were carried out, studying the mechanical behaviour of masonry infilled framed structures. For example, an experimental study carried out by Smith (1996) (Smith 1966) showed that when testing inflexible frames the first signs of cracking occur along the compression diagonal of the infill wall. Other researchers such as (Mainstone 1971) and (Focardi & Manzini 1984) investigated the failure mechanisms in framed masonry infilled walls. From such studies, the following types of cracking could occur: localized crushing at the corners closest to the applied load; diagonal cracking; sliding through the mortar joint; and a combination of diagonal cracking and sliding cracking. Figure 1 illustrates in-plane failure modes of infilled frames.

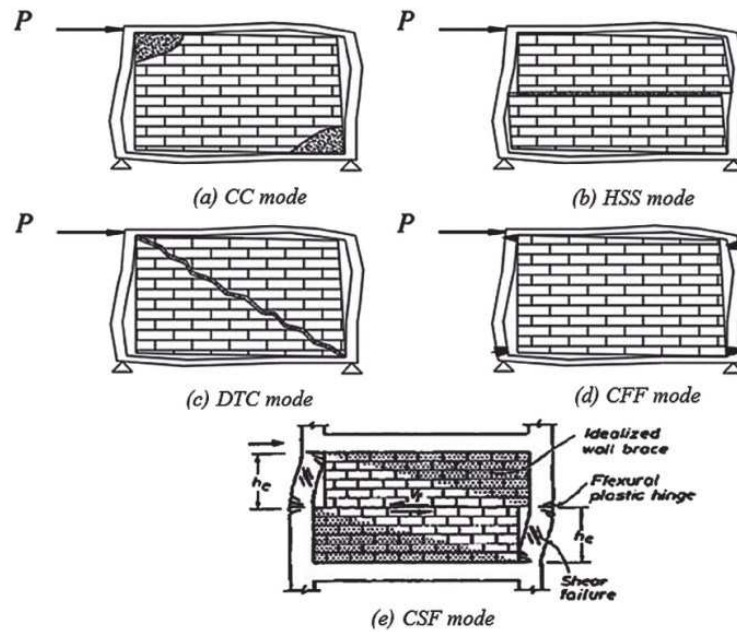


Figure 1. In-plane failure modes of infilled frames: (a) corner crushing (CC) mode; (b) horizontal sliding shear (HSS) mode; (c) diagonal tension cracking (DTC) mode; (d) column flexural failure (CFF) mode (El Dakhakhni et al. 2003); and (e) column shear failure (CSF) mode (Paulay & Priestley 1992).

However, as experimental research is prohibitively expensive, it is fundamentally important to have available a computational model that can be used to predict mechanical behaviour of masonry infilled RC framed structures. Over the last four decades, several computational modelling strategies have been developed to investigate the mechanical behaviour of masonry infilled RC frame structures. One of the most common strategies is the macromodelling approach in which the masonry infill wall is replaced by an equivalent pinned strut with the same material and thickness as that of the masonry infill wall (Figure 2).

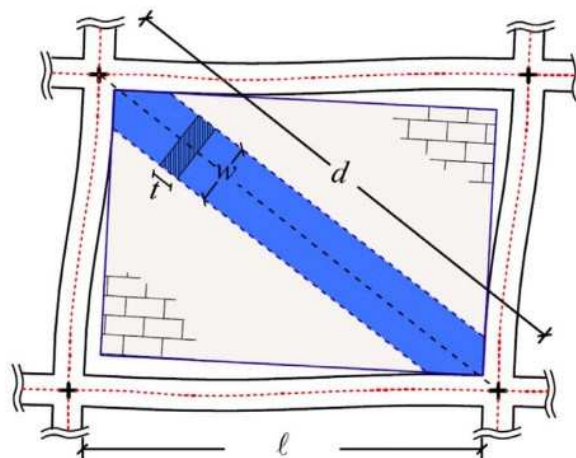


Figure 2. Equivalent pinned strut (Cavaleri et al. 2017).

Past studies by (Dolšek & Fajfar 2008) and (Papia et al. 2003) highlighted that the response of the composite system is highly sensitive to the equivalent strut width and strength of the masonry infill wall. Therefore, the selection of an accurate constitutive law for the representation of the strut is essential to accurately predict the mechanical behaviour of the masonry infilled RC frame structure (Asteris et al. 2015; Cavaleri & Di Trapani 2014; Saneinejad & Hobbs 1995; Mainstone 1974; Mainstone 1971). An alternative strategy for predicting the mechanical behaviour of masonry infilled frame systems is that characterized by the finite element (FE) micromodelling approach (Koutromanos & Shing 2012; Koutromanos et al. 2011; Asteris 2003). The FE micromodelling approach can simulate the behaviour of the infills and the RC frames. Masonry infill walls are represented by two-dimensional or three-dimensional FEs with equivalent geometry to that of the structure to be simulated. The surrounding of the masonry infill walls frame is modelled using beam elements. In addition, the interaction between the masonry infill walls and the frame can also be simulated using ad-hoc FEs. Although this computational modelling strategy is the most accurate, since it closely represents the physical system under investigation, it requires large computational effort in terms of time and material properties to be inputted into the model. (Mehrabi & Shing 1997) proposed a smeared-crack FE model to investigate the mechanical behaviour of masonry infilled RC framed structures. Later, (Moghadam 2004) and (Moghadam et al. 2006) developed an analytical approach for the shear strength and crack pattern evaluation for masonry infill walls. The approach was based on the minimization of the failure surface in a masonry infill walls. (Stavridis 2009) and (Stavridis & Shing 2010) proposed a model combining smeared and discrete crack approaches. The model could capture the different failure modes in infilled frames with sufficient accuracy. A year later, (Koutromanos et al. 2011) extended the work of (Stavridis & Shing 2010) and implemented a cohesive crack interface model as well as an improved smeared-crack model to capture the cyclic behaviour of infilled frames. The discrete element method (DEM) of analysis is an alternative to the FE-based approaches. This approach can be used to simulate the non-linear behaviour of masonry infilled frames and investigate the discontinuous nature of the masonry infill wall as well as the interaction between the frame and the masonry infill wall. Two-dimensional micromodelling using DEM to investigate the non-linear lateral load behaviour of confined masonry walls and masonry infilled frames under monotonic loading has been developed by (Sarhosis et al. 2014; Mohebbkhah et al. 2008; Mohebbkhah & Tasnimi 2007). Extensive reviews on numerical micromodelling aspects of masonry infilled frames and masonry structures have been presented in (Asteris et al. 2016; Asteris et al. 2013), respectively.

One of the main topics that many researchers have tried to understand is that of the influence of the size and location of openings in masonry infilled frame structures (e.g., Sigmund & Penava 2014; Decanini et al. 2014; Asteris et al. 2012; Kakaletsis & Karayannis 2009; Kakaletsis & Karayannis 2008; Kakaletsis & Karayannis 2007). Dawe and Young (1985) and Penava (2012) (Penava 2012; Dawe & Young 1985) investigated experimentally the influence of openings in the masonry infill wall

on the lateral resistance of the frame. They found that at low drift levels (e.g., 1%), masonry infilled walls containing openings do not influence the initial stiffness and strength of the framed masonry. However, at higher drift levels (e.g., 2%), the presence of openings lowers the energy dissipation capacity of the system. They also observed that the failure mechanism is highly dependent on the location and size of the opening. Several numerical models have also been used to investigate the influence of the size and location of the openings in masonry infilled frame structures (Gazić & Sigmund 2013; Sigmund & Penava 2013; Asteris et al. 2011; Crisafulli & Carr 2007; Moghadam et al. 2006; Crisafulli et al. 2005; Al-Chaar et al. 2003; Crisafulli et al. 2000; Saneinejad 1990; Negro & Colombo 1997; Mehrabi & Shing 1997; Achyutha et al. 1986).

From such studies it was shown that, as the size of the opening was increased, the overall stiffness of the system reduced. When the size of the opening exceeds 50% of the infill wall size, the stiffness factor remains relatively constant. Additionally, when the position of the opening is moved towards the compression diagonal of the infill wall, the action of the frame and the infill wall is adversely affected. However, today, it is questionable to what extent the individual components (i.e., the masonry infill wall and the RC frame) contribute to the lateral resistance of the frame, and whether openings provide beneficial (positive) effects or disruptive effects leading to an increase in the vulnerability of the structure (Sozen 2014; Shimazaki & Sozen 1984; Fiorato et al. 1970).

The aim of this paper is to draw upon the significance of the opening type, size and position on the lateral load carrying capacity of masonry infilled RC frame structures and investigate the contribution of masonry infilled walls (with and without openings) and RC frames on the lateral response of the structure. A computational model based on the non-linear FE method of analysis has been developed. The model can study the non-linear interaction between masonry infill walls and RC frames. Initially, the developed computational model was validated against a series of 1/2.5 scale experimental tests carried out in the laboratory. Next, a series of parametric studies was carried out to investigate the influence of opening size (e.g., windows and doors) on the lateral stiffness of the masonry infilled RC frame structures. The internal shear forces in the masonry infill wall and RC frames of framed-wall systems at various damage grades were computed. These were then compared with corresponding bare frames and expressed as shear resistance capacity demand.

2 Description of experimental tests

Ten 1/2.5 scaled masonry infilled RC frame structures were constructed and tested in the laboratory (Table 1). Frames were designed using medium-ductility level of seismic detailing (DCM) in compliance with EN 1992-1-1 (CEN 2004a) and EN 1998-1 (CEN 2004b). Masonry infill wall was

made of Group 2 clay block masonry units (Figure 3) bonded together with M5 class designation mortar joints in compliance with EN 1996-1-1 (CEN 2005).

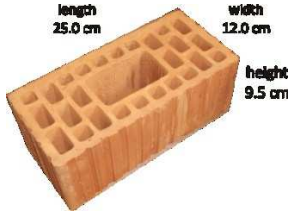


Figure 3. Clay block masonry units used in the experimental study to construct the masonry infill wall.

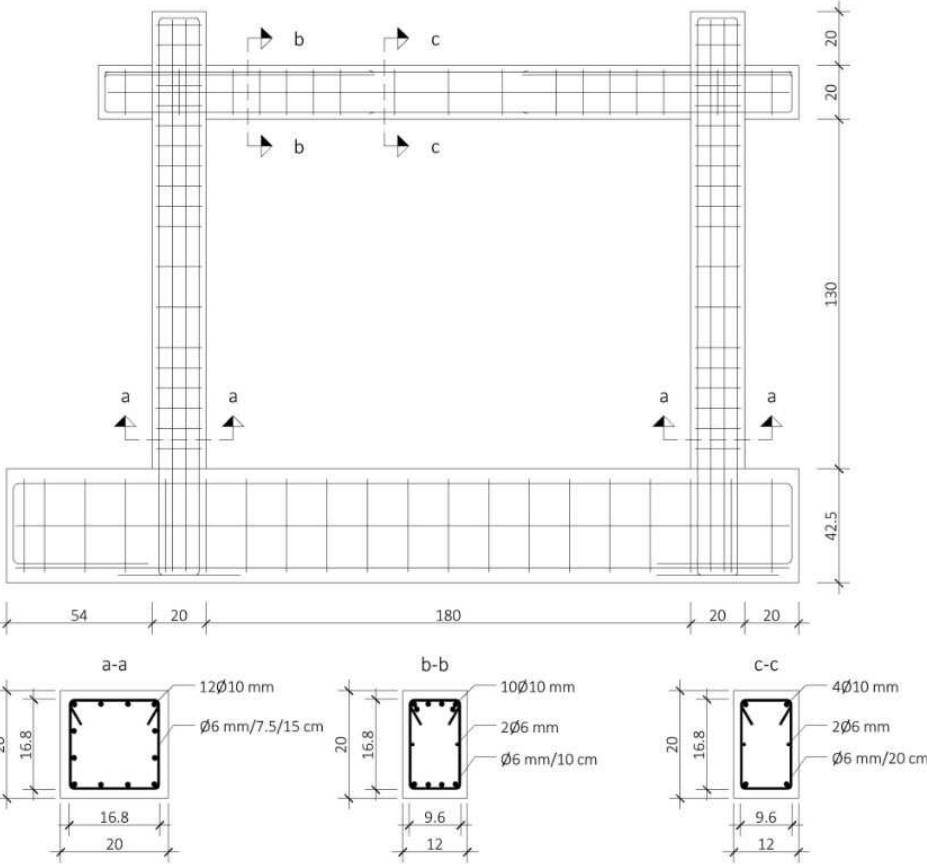








Figure 4. Reinforced concrete frames with masonry infill walls in the laboratory (Penava 2012).

Specimens were preloaded with a constant vertical load equal to 365 kN, which was applied at the column-ends. Quasi-static cyclic lateral loading was applied at the beam-ends (see Fig. 4). When the masonry infill wall reached significant damage (DG 3-EMS 98), static pushover loading was applied up to total collapse (Grünthal et al. 1998). Test specimens were divided into two groups (see Table 1). The first group consisted of four specimens with an unconfined opening (i.e., a door or window) position either centrally or eccentrically. The second group had two reference specimens. These included an infilled frame without an opening and a bare RC frame. Dimensions of the different test specimens are shown in Figure 4 and Table 1.

Table 1. Classification and description of the specimens tested in the laboratory.

Specimen		Appearance of the specimen	Opening		Description
Group	Mark		Type and area	Position	
I	1		Door $l_o/h_o=0.35/0.90$ m $A_o=0.32$ m ² $A_o/A_i=0.14$	Centric $e_o=l_i/2=0.90$ m	Specimens without confinement
	2		Window $l_o/h_o=0.50/0.60$ m $A_o=0.30$ m ² $A_o/A_i=0.13$	Centric $e_o=l_i/2=0.90$ m $P=0.40$ m	
	3		Door $l_o/h_o=0.35/0.90$ m $A_o=0.32$ m ² $A_o/A_i=0.14$	Eccentric $e_o=h_i/5+l_o/2=0.44$ m	
	4		Window $l_o/h_o=0.50/0.60$ m $A_o=0.30$ m ² $A_o/A_i=0.13$	Eccentric $e_o=h_i/5+l_o/2=0.44$ m $P=0.40$ m	
II	1		-	-	Reference specimens
	2		-	-	

Notations:

A_o is the area of an opening and is equal to the height of the opening (h_o) multiplied by the length of the opening (l_o);

A_i is the area of the masonry infill wall and is equal to the height of the masonry infill wall (h_i) multiplied by the length of the masonry infill wall (l_i);

h_i is equal to 1.3 m;

l_i is equal to 1.8 m;

e_o is the eccentricity of the opening;

t_i is the masonry infill wall thickness and is equal to 0.12 m;

For the different specimens tested in the laboratory, graphs of their shear resistance against displacement have been produced. The sequenced failure mechanism of the masonry infill wall in the case of an opening without confinement was also recorded. A detailed description of the experimental testing campaign and results can be found in (Penava 2012) and (Sigmund & Penava 2014). Results of such experimental tests have been used for the validation of the computational model that is described in Section 3.

3 Development of the computational model

To describe the non-linear behaviour of masonry infilled RC frames tested in the laboratory, a computational model based on the simplified micromodelling approach has been developed. The commercial two-dimensional FE software ATENA 2D Eng (Cervenka Consulting s.r.o. 2015) was used.

3.1 Development of the geometric models

Geometric models were created to represent the masonry infilled RC frame structures constructed in the laboratory. Masonry units and the mortar–masonry interface were considered separately. Each brick of the masonry infill wall was represented by a block separated by zero thickness interfaces at each mortar bed and head joint. To allow for the thick mortar joints in the real masonry infill walls, each masonry unit was based on the nominal brick size increased by half of the thickness of the mortar joint in each face direction (Figure 5). Cracking in masonry units and concrete frame has been modelled by the smeared crack approach (Pryl & Cervenka 2013; Cervenka et al. 2012).

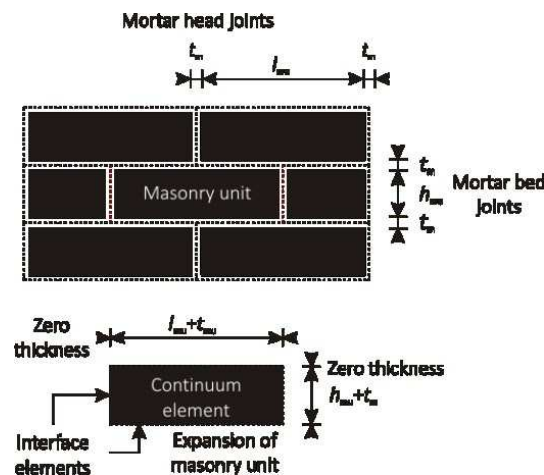


Figure 5. Simplified micromodelling approach used.

The structural system was assembled by using iso-parametric plane FEs (9-node quadrilateral and 6-node triangular) for concrete and masonry units, and truss elements (3-nodes) for reinforcement and gap elements with non-linear geometry for the interface. Mesh convergence tests were carried out and an FEs mesh, with an element length equal to one quarter of the structural element size, was assigned in the model. A typical geometric model of the masonry infilled RC frame was developed in ATENA 2D Eng and is shown in Figure 6.

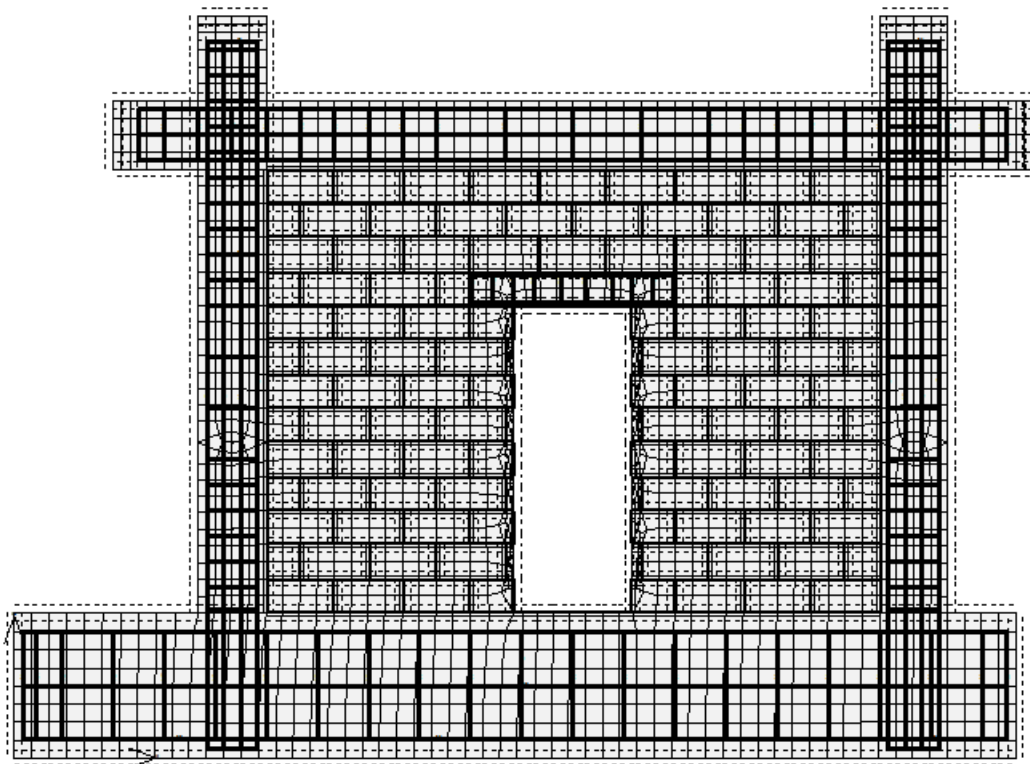


Figure 6. Typical masonry infilled reinforced concrete frame developed in ATENA 2D Eng (Cervenka Consulting s.r.o. 2015).

3.2 Constitutive laws and material properties

The fracture-plastic constitutive law, known as the NonLinCementitious2 material model based on the rotated crack approach, was adopted for the RC frame and the lintel (Cervenka et al. 2012). The input material parameters used are shown in Table 2. These were obtained from (Cervenka et al. 2012). Longitudinal and transversal steel reinforcements were modelled as truss elements based on the Menegotto–Pinto model with a bi-linear primary curve with strain hardening (Cervenka et al. 2012). Bond-slip of the reinforcement was neglected in the calculations. Material properties for the

reinforcement were obtained from (Bažant & Planas 1997; Bažant & Chern 1985; Bažant & Oh 1983a; Bažant & Oh 1983b) and are shown in Table 3. For the reinforced concrete lintel, the concrete compressive strength was estimated by conducting tests in compliance with EN 12390-3 (CEN 2009). The concrete compressive strength was equal to 30 MPa. For the RC elements, the transverse reinforcement bar closest to the joint moved further away from the joint edge, while its area was increased by about 100 times to prevent unrealistic tension softening. In the case of a high reinforcement ratio in the plastic hinge region, tension stiffening and the maximum crack spacing parameters for the concrete material were used. Due to large vertical pre-compression, the effect of friction was taken into consideration. For introducing friction force on to the numerical model, a non-linear surface spring was set on the beams end on the opposite side of the in-plane applied loading. The friction force for one column end was calculated to be 10 kN (Anić et al. 2017). For the clay block masonry units, with vertical hollows, the interface link element had to facilitate an additional cohesion hardening–softening function (see Figure 7) (Penava et al. 2016a). This was due to the mortar interlocking, which prevented shear sliding failure until tension failure of the unit occurred; this is defined as the limit shear strength in EN 1996-1-1 (CEN 2005). The corresponding deformation evaluated was based on the unit shear modulus, because the clay block unit was brittle and exhibited linear elastic behaviour until shear failure. For solid surfaces (perpendicular to the hollows or in the case of solid clay blocks), this additional function for modelling the cohesion was not necessary. As an orthotropic material model for the masonry unit was not available, different levels of stiffness in orthogonal directions were modelled using different values for head and bed joint stiffness. These were evaluated based on the masonry unit’s values for the elastic modulus in corresponding directions. When combined with the interlocking of the mortar and units, this led to overcoming an effect in which the units were pushed, rather than crushed, in the numerical model. This behaviour was opposite to the one observed in the experiments. This phenomenon was especially pronounced in the case of an opening in the masonry wall when combined with a bed joint sliding failure mechanism (Penava et al. 2016a; Penava et al. 2016b).

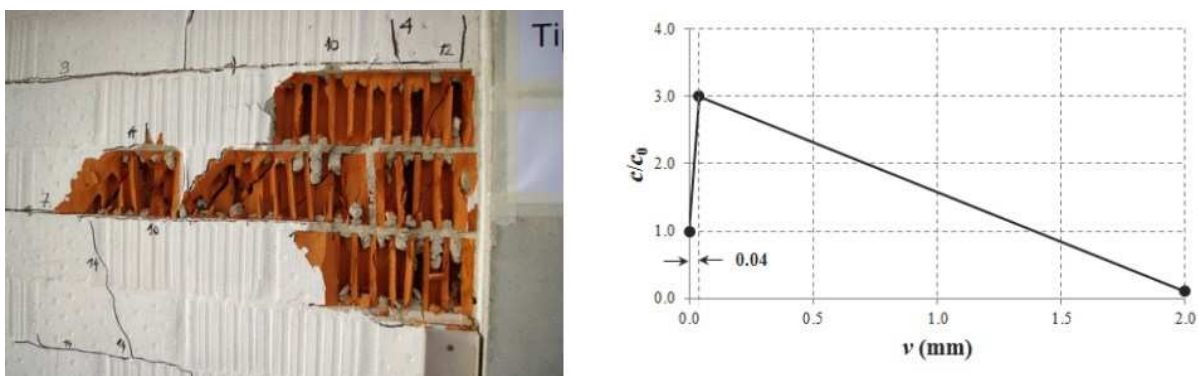


Figure 7. (a) Mortar interlocking with the units; and (b) cohesion hardening–softening function.

Table 2. Concrete properties for material model NonLinCementitious2.

Description	Symbol	Value	Units
Elastic modulus	E	41000	MPa
Poisson's ratio	μ	0.2	-
Tensile strength	f_t	4	MPa
Compressive strength	f_c	-58	MPa
Specific fracture energy	G_f	$1.20 \cdot 10^{-4}$	MN/m
Critical compressive displacement	w_d	$-1.0 \cdot 10^{-3}$	m
Eccentricity, defining the shape of the failure surface	E_{xc}	0.52	-
Multiplier for the direction of the plastic flow	β	0	-
Crack model coefficient (1.0 for Fixed, 0.0 for Rotated)	-	0	-
Plastic strain at compressive strength	ϵ_{CP}	$-1.417 \cdot 10^{-3}$	-
Reduction of compressive strength due to cracks	$f_{c,LIM}$	0.1	-
Crack shear stiffness factor	s_F	20	-
Aggregate size	-	0.016	m
Crack spacing	s_{max}	0.125	m
Tension stiffening	c_{ts}	0.4	-

Table 3. Reinforcement properties for cycling reinforcement.

Description	Symbol	Value	Units
Elastic modulus	E	210000	MPa
Yield strength	σ_y	550	MPa
Ultimate strength	σ_t	650	MPa
Strain at ultimate strength	ϵ_{lim}	0.01	-
Bauschinger effect exponent	R	20	-
Menegotto–Pinto model parameter	$C1$	0.925	-
Menegotto–Pinto model parameter	$C2$	0.15	-

For the representation of the quasi-brittle nature of the clay block masonry units, the rotated crack model based on SBeta material model (Cervenka et al. 2012) has been used. Due to the orthotropic nature of masonry, different properties for the head and bed mortar joints were assigned. Table 4 shows the properties of masonry units. The contact between the masonry units, as well as between the masonry units and the frame, was described by the interface material model. Mortar joints were represented as zero thickness interfaces based on the Mohr–Coulomb criterion with tension cut-off. Normal (K_{nn}) and shear (K_{tt}) stiffness calculated using the expressions

(1) and (2) from (Pryl & Cervenka 2013; Cervenka et al. 2012). The properties of bed and head joints are given separately in Tables 5 and 6, respectively.

$$K_{nn} = E/t \quad (1)$$

$$K_{tt} = G/t \quad (2)$$

where E and G are the modulus of elasticity and the shear modulus of the masonry unit, and t is the thickness of the mortar joint.

Table 4. Properties of the clay block masonry unit.

Description	Symbol	Value	Units
Elastic modulus parallel to the head joints	E_{hj}	5650	MPa
Elastic modulus parallel to the bed joints	E_{bj}	850	MPa
Poisson's ratio	μ	0.1	-
Tensile strength	f_t	1.8	MPa
Compressive strength parallel to the head joints	f_c	-17.5	MPa
Compressive strength parallel to the bed joints	f_c	-2.8	MPa
Type of tension softening	Exponential		
Specific fracture energy	G_f	$0.45 \cdot 10^{-4}$	MN/m
Crack model	Rotated		
Compressive strain at compressive strength in the uniaxial compressive test	ε_c	$-1.358 \cdot 10^{-3}$	-
Reduction of compressive strength due to cracks	-	0.8	-
Type of compression softening	Crush Band		
Critical compressive displacement	w_d	$-5.0 \cdot 10^{-4}$	m
Shear retention factor	Variable		
Tension–compression interaction	Linear		

Table 5. Initial properties of bed joints.

Description	Symbol	Value	Units
Normal stiffness	K_{nn}	$5.65 \cdot 10^5$	MN/m ³
Tangential stiffness	K_{tt}	$2.57 \cdot 10^5$	MN/m ³
Cohesion	C	0.35	MPa
Tensile strength	f_t	0.2	MPa
Friction coefficient	-	0.24	-
Minimum normal stiffness	$K_{nn,min}$	$5.65 \cdot 10^2$	MN/m ³
Minimum tangential stiffness	$K_{tt,min}$	$2.57 \cdot 10^2$	MN/m ³
Function tension softening–hardening	Not used		

Table 6. Initial properties of head joints.

Description	Symbol	Value	Units
Normal stiffness	K_{nn}	$8.50 \cdot 10^4$	MN/m ³
Tangential stiffness	K_{tt}	$3.86 \cdot 10^4$	MN/m ³
Cohesion			
Tensile strength	Adopted from the bed joints		
Friction coefficient			
Minimum normal stiffness	$K_{nn,min}$	$8.50 \cdot 10^1$	MN/m ³
Minimum tangential stiffness	K_{ttmin}	$3.86 \cdot 10^1$	MN/m ³

3.3 Boundary conditions and application of external applied load

Displacement and force boundary conditions were selected to correspond with those from the tests (direct shear), including the use of a fixed-base beam and the prevention of vertical movement in the column-ends. Forces were applied at the beam-ends. The vertical load was applied in five steps until the target value was achieved. The horizontal load was then applied in increments of 10kN. Steel pads (plane FEs with a linear elastic constitutive law) were placed at the beam- and column-ends, as in the tests.

3.4 Verification of the computational model

For the verification of the numerical model, computational models of the bare frame specimen (Specimen II/1), the infilled frame specimen (Specimen II/2), and the infilled specimens with openings were developed and the results compared against those obtained from the experiments (see Section 2). Comparison of the computational results with the experimental results are shown in Figure 8. Results are presented using response envelope (primary) curves. In Figure 8, displacements (d) and drift ratios ($d_r = d/h_i + h_b/2$ where h_b is beam height) are presented on the horizontal axis, while base shear resistance (V_R) and normalized base shear resistance ($V_R/V_{R,max,f}$ where $V_{R,max,f}$ is base shear resistance of the bare frame) appear on the vertical axis. Observed failure mechanisms are given for the pushover direction in Figure 9. From Figure 9, the difference between the numerical and experimental results (differences) were within the range of acceptable tolerance (error <15%). The developed computational model could predict the failure mode of the masonry infilled reinforced concrete frame specimens with sufficient accuracy.

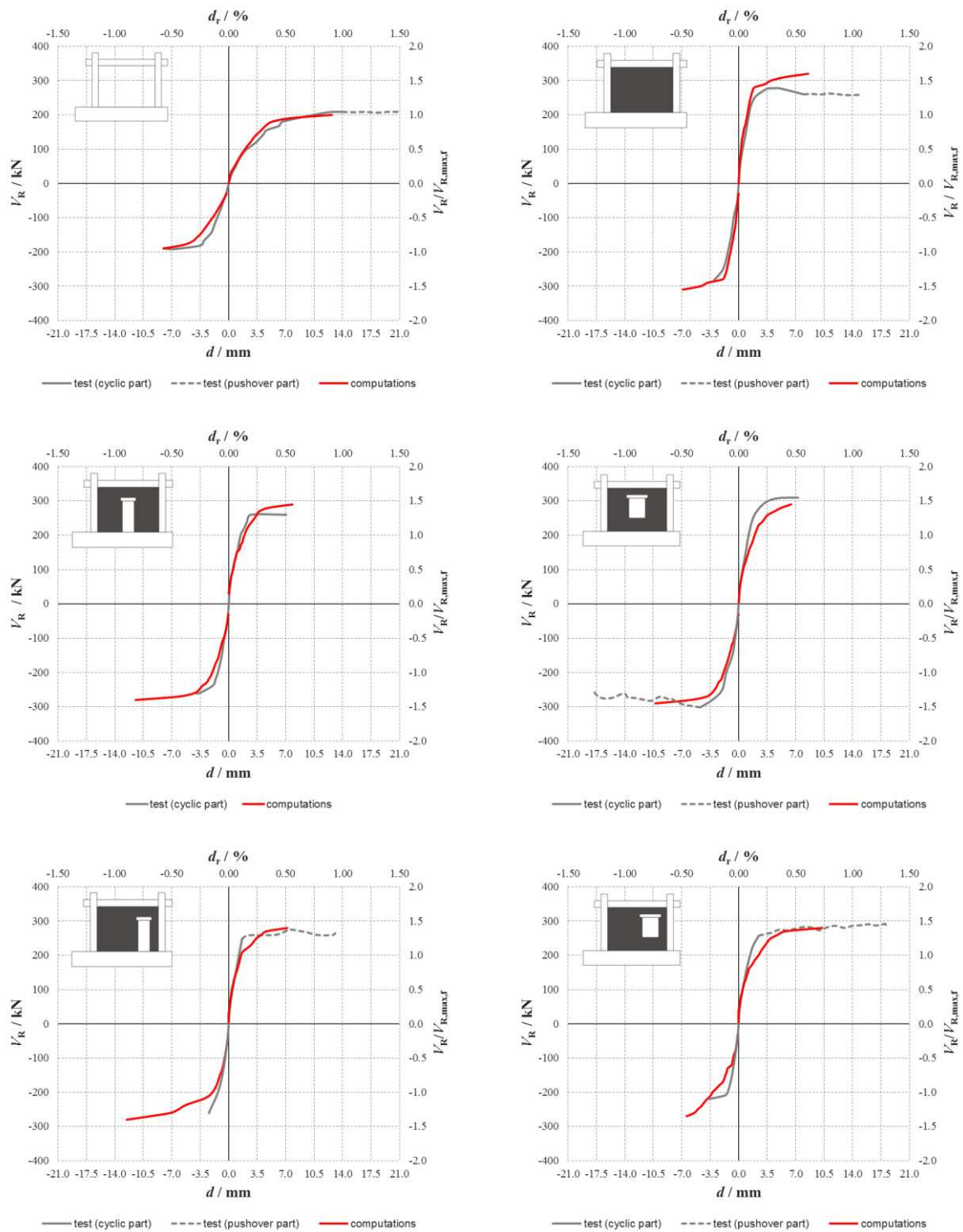


Figure 8. Comparison of experimental with computational resistance envelope curves for the different specimens tested in the laboratory.


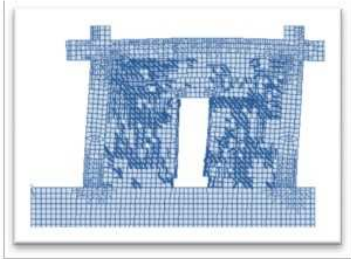

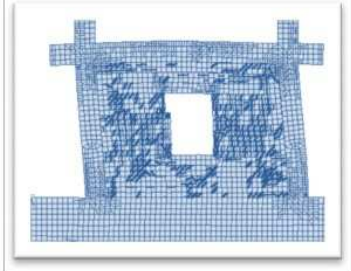

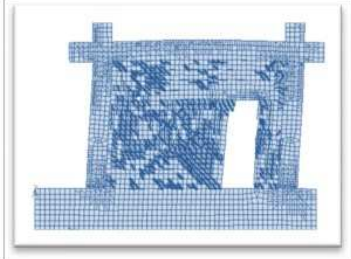

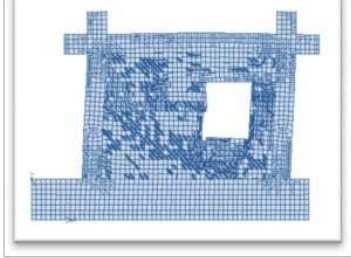

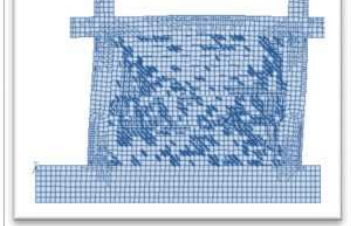
Spec.	Failure mechanism description	Experiment (Penava 2012)	Computations (ATENA2D Eng)
I/1	Sequenced (multiple): 1. Bed joint sliding above opening 2. Diagonal tensile failure of masonry pier		
I/2	Sequenced (multiple): 1. Bed joint sliding above opening 2. Diagonal tensile failure of masonry pier		
I/3	Sequenced (multiple): 1. Bed joint sliding above opening 2. Diagonal tensile failure of masonry pier		
I/4	Sequenced (multiple): 1. Bed joint sliding above and below opening 2. Bed joint sliding of masonry pier		
III/2	Bed joint sliding		

Figure 9. Comparison of computational with experimental failure mechanisms of reinforced concrete frames with masonry infill wall specimens.

4 Parametric study on masonry infill containing openings

An extensive parametric study has been carried out to assess the shear resistance of frame-wall systems containing different sizes and positions of openings. The previously described calibrated simplified micromodel was used. Differently sized door and window openings were positioned centrally or eccentrically in the masonry infill wall. The opening sizes investigated in this study cover those most commonly used in construction practice (Neufert & Neufert 2012) and were classified as “medium size” when the opening to infill wall area ratio ranged from 7.5 to 15%, i.e., $7.5\% \leq A_o/A_i \times 100 \leq 15\%$; “large size” when $A_o/A_i \times 100 > 15\%$; and “small size” when $7.5\% < A_o/A_i \times 100$. Small size openings were not considered in this study since they do not significantly affect the shear resistance response compared with the response of the infilled frame without openings (Penava 2012). With respect to opening position, the following two cases were investigated:

- (i) Centrally positioned openings $e_o = l_i/2$;
- (ii) Eccentrically positioned openings $e_o = h_i/5 + l_o/2$

where e_o was the distance measured from the inner side of the right frame column, l_i infill wall length, h_i infill wall height and l_o opening length. For infill walls with eccentric openings, a loading was applied both from left to the right (i.e., in the positive direction) and right to left (i.e., in the negative direction). A complete list of the different computational studies undertaken is shown in Table 7 and Table 8.

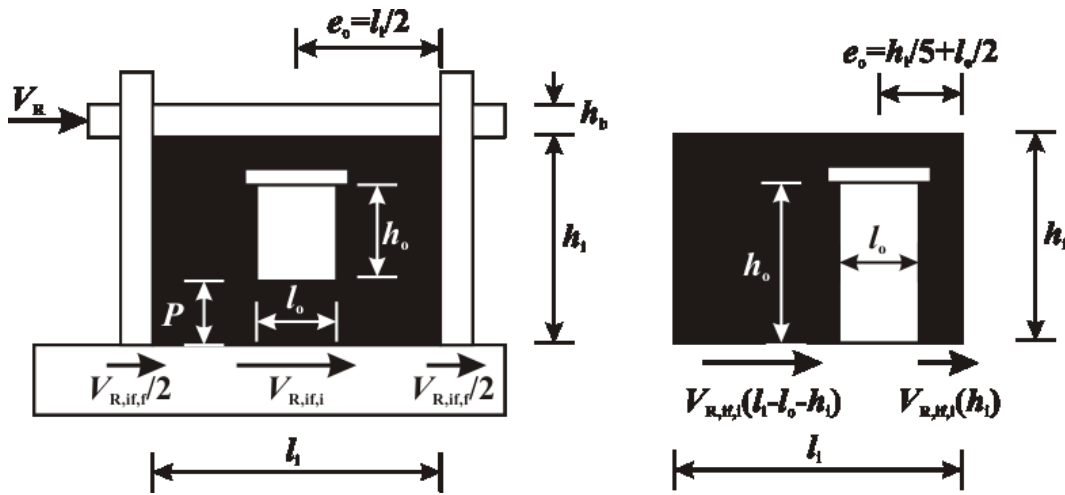


Figure 10. Explanation of symbols used.

The frame-wall system was subjected to a displacement controlled non-linear static (pushover) analysis. This was to account for the resistance response after the highest value of shear resistance $V_{R,max}$ was reached. A limit drift ratio (d_r) equal to 2% was selected in compliance with the damage limitation criteria for frame member (CEN 2004b). The shear resistances of the infilled wall and RC

columns were recorded in the level of column's feet as the potential plastic hinge (shear failure) location. The shear resistance values in the frame $V_{R,if,f}$ (kN) and the infill wall $V_{R,if,I}$ (kN) member of the infilled frame system was compared with the shear resistance of the frame without infill wall case (bare frame) $V_{R,f}$ (kN) at various displacement d (mm) i.e. drift ratio d_r (%) values, namely 0.10, 0.25, 0.5, 0.75, 1.0, 1.25, 1.5, 1.75 and 2%. The drift ratios correspond to the predefined damage grades 1 to 5 which are based on EMS-98 damage scale (Grünthal et al., 1998) and occurred within the masonry infill. The damage grades are:

- Grade 1: Negligible to slight damage (no structural damage, slight non-structural damage) at d_r equal to 0.1%;
- Grade 2: Moderate damage (slight structural damage, moderate non-structural damage) at d_r ranges from 0.2 to 0.4%;
- Grade 3: Substantial to heavy damage (moderate structural damage, heavy non-structural damage) at d_r equal to 0.5%;
- Grade 4: Very heavy damage (heavy structural damage, very heavy non-structural damage) at d_r ranges from 0.75 to 1.0%;
- Grade 5: Destruction (very heavy structural damage) at d_r equal to 2.0%.

The value of each of the member resistances was additionally expressed through the normalized shear resistance, e.g., $V_{R,if,f} / V_{R,max,f}$ or $V_{R,if,I} / V_{R,max,f}$, where $V_{R,max,f}$ stands for the highest shear resistance of the bare frame.

Table 7. Description and classification of the window openings cases.

Type	Mark	Measures and area	Position		Size
Window	8×12	$l_o/h_o = 0.40/0.60$ m $P=0.40$ m $A_o = l_o * h_o = 0.24$ m ² $A_o/A_i * 100 = 10.3$ %	Centric $e_o = l_i/2 = 0.90$ m	Eccentric $e_o = h_i/5 + l_o/2 = 0.46$ m	Medium $A_o/A_i * 100 \leq 15\%$
	10×12	$l_o/h_o = 0.50/0.60$ m $P=0.40$ m $A_o = l_o * h_o = 0.30$ m ² $A_o/A_i * 100 = 12.8\%$	Centric $e_o = l_i/2 = 0.90$ m	Eccentric $e_o = h_i/5 + l_o/2 = 0.51$ m	
	12×12	$l_o/h_o = 0.60/0.60$ m $P=0.40$ m $A_o = l_o * h_o = 0.36$ m ² $A_o/A_i * 100 = 15.4\%$	Centric $e_o = l_i/2 = 0.90$ m	Eccentric $e_o = h_i/5 + l_o/2 = 0.56$ m	Large $A_o/A_i * 100 > 15\%$
	16×12	$l_o/h_o = 0.80/0.60$ m $P=0.40$ m $A_o = l_o * h_o = 0.48$ m ² $A_o/A_i * 100 = 20.5\%$	Centric $e_o = l_i/2 = 0.90$ m	Eccentric $e_o = h_i/5 + l_o/2 = 0.66$ m	

Table 8. Description and classification of the door opening cases.

Type	Mark	Measures and area	Position		Size
Door	6×16	$l_o/h_o = 0.30/0.80$ m $A_o = l_o * h_o = 0.24$ m ² $A_o/A_i * 100 = 10.3\%$	Centric $e_o = l_i/2 = 0.90$ m	Eccentric $e_o = h_i/5 + l_o/2 = 0.41$ m	Medium $A_o/A_i * 100 \leq 15\%$
	7×16	$l_o/h_o = 0.35/0.80$ m $A_o = l_o * h_o = 0.28$ m ² $A_o/A_i * 100 = 12.3\%$	Centric $e_o = l_i/2 = 0.90$ m	Eccentric $e_o = h_i/5 + l_o/2 = 0.435$ m	
	8×16	$l_o/h_o = 0.40/0.80$ m $A_o = l_o * h_o = 0.32$ m ² $A_o/A_i * 100 = 13.7\%$	Centric $e_o = l_i/2 = 0.90$ m	Eccentric $e_o = h_i/5 + l_o/2 = 0.46$ m	
	6×18	$l_o/h_o = 0.30/0.90$ m $A_o = l_o * h_o = 0.27$ m ² $A_o/A_i * 100 = 11.5\%$	Centric $e_o = l_i/2 = 0.90$ m	Eccentric $e_o = h_i/5 + l_o/2 = 0.41$ m	
	7×18	$l_o/h_o = 0.35/0.90$ m $A_o = l_o * h_o = 0.315$ m ² $A_o/A_i * 100 = 13.5\%$	Centric $e_o = l_i/2 = 0.90$ m	Eccentric $e_o = h_i/5 + l_o/2 = 0.435$ m	
	10×16	$l_o/h_o = 0.50/0.80$ m $A_o = l_o * h_o = 0.40$ m ² $A_o/A_i * 100 = 17.1\%$	Centric $e_o = l_i/2 = 0.90$ m	Eccentric $e_o = h_i/5 + l_o/2 = 0.46$ m	Large $A_o/A_i * 100 > 15\%$
	12×16	$l_o/h_o = 0.60/0.80$ m $A_o = l_o * h_o = 0.48$ m ² $A_o/A_i * 100 = 20.5\%$	Centric $e_o = l_i/2 = 0.90$ m	Eccentric $e_o = h_i/5 + l_o/2 = 0.51$ m	
	16×16	$l_o/h_o = 0.80/0.80$ m $A_o = l_o * h_o = 0.64$ m ² $A_o/A_i * 100 = 27.4\%$	Centric $e_o = l_i/2 = 0.90$ m	Eccentric $e_o = h_i/5 + l_o/2 = 0.66$ m	
	8×18	$l_o/h_o = 0.40/0.90$ m $A_o = l_o * h_o = 0.36$ m ² $A_o/A_i * 100 = 15.4\%$	Centric $e_o = l_i/2 = 0.90$ m	Eccentric $e_o = h_i/5 + l_o/2 = 0.46$ m	
	10×18	$l_o/h_o = 0.50/0.90$ m $A_o = l_o * h_o = 0.45$ m ² $A_o/A_i * 100 = 19.2\%$	Centric $e_o = l_i/2 = 0.90$ m	Eccentric $e_o = h_i/5 + l_o/2 = 0.51$ m	
	12×18	$l_o/h_o = 0.60/0.90$ m $A_o = l_o * h_o = 0.54$ m ² $A_o/A_i * 100 = 23.1\%$	Centric $e_o = l_i/2 = 0.90$ m	Eccentric $e_o = h_i/5 + l_o/2 = 0.56$ m	
	16×18	$l_o/h_o = 0.35/0.80$ m $A_o = l_o * h_o = 0.72$ m ² $A_o/A_i * 100 = 30.8\%$	Centric $e_o = l_i/2 = 0.90$ m	Eccentric $e_o = h_i/5 + l_o/2 = 0.66$ m	

4.1 Bare frame and full infill frame

The seismic capacity of a bare frame and that of an infill frame with no openings was investigated. Figure 11 shows the shear resistance against drift ratio for the bare frame (left) and infill frame with no opening (right). In Figures 11 to 21, “frame” refers to the bare frame; “infilled frame (frame)” refers to the sum of the internal shear forces at the feet of the RC columns of the frame; and “infilled frame

(infill)” refers to the sum of internal shear forces along the length at the base of the infill wall. From Figure 11a, for the bare frame, the maximum shear resistance at the columns’ feet is equal to 210 kN at 0.75% drift ratio. For the infill frame without openings (Figure 11b), the maximum shear resistance at the columns’ feet is equal to 194 kN at 0.75% drift ratio, while the maximum shear resistance of the infill wall is equal to 197 kN at 0.25% drift ratio. Thus, it is evident that the infill frame is much stiffer when compared with the bare frame because the masonry infill is confined by the RC columns, which adds to its resistance.

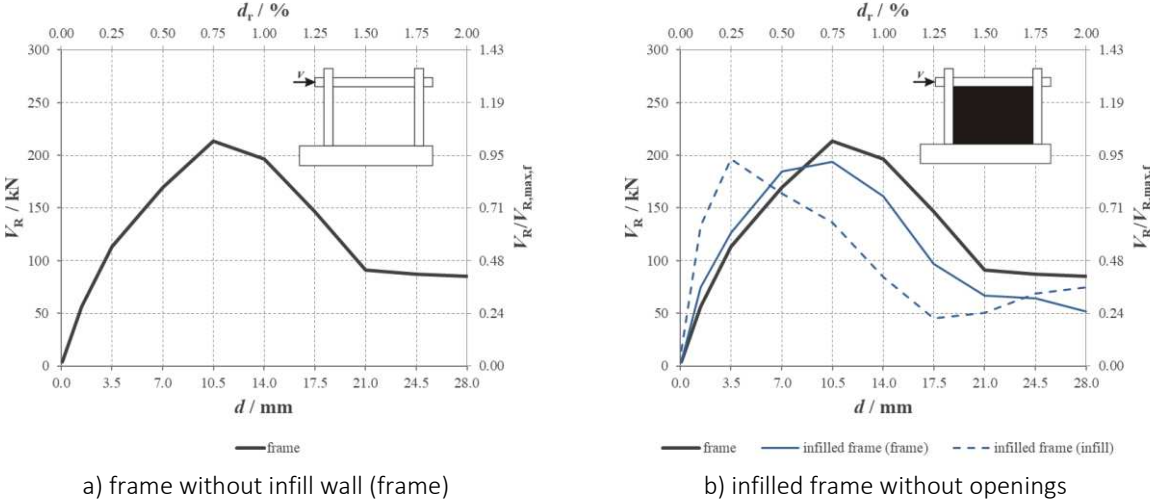


Figure 11. Shear resistance at (a) the feet of the reinforced concrete (RC) frame of a bare RC frame; and (b) the base of the masonry infill wall of an infilled frame with no openings.

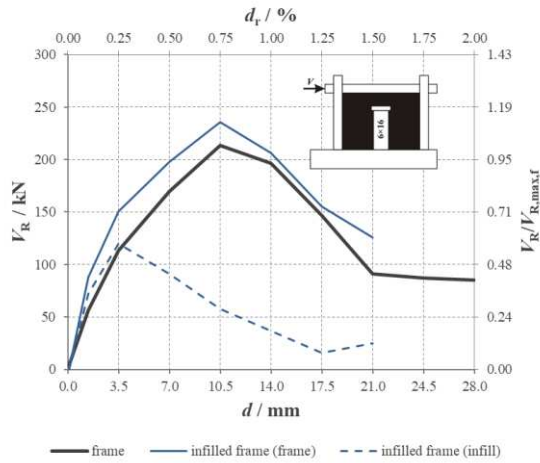
4.2 Masonry infill with centrally positioned doors

4.2.1 Masonry infill with medium size door opening positioned centrally

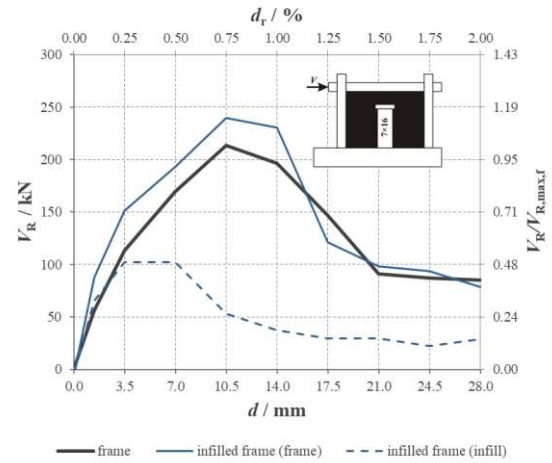
Figure 12 shows the masonry infill and frame columns’ shear resistance against drift ratio for the medium size door opening positioned centrally. For medium size centrally positioned door openings, the maximum shear resistance of the columns of the frame increases by 9 to 12% when compared with the bare frame. The maximum shear resistance of the infill wall also reduces 40 to 49% when compared with the masonry infill wall with no opening. When the percentage of the area of the opening over the area of the infill (A_o/A_i*100) is 10.3% (Figure 12a), the maximum shear resistance at the feet of the RC columns of the frame is equal to 236 kN at 0.75% drift ratio and the maximum shear resistance at the base of the masonry infill wall is equal to 120 kN at 0.25% drift ratio. Similarly, when A_o/A_i*100 is equal to 13.7% (Figure 12b), the maximum shear resistance at the feet of the columns of the frame is equal to 240 kN at 0.75% drift ratio while the maximum shear resistance of the infill wall is equal to 109 kN at 0.25% drift ratio. However, when A_o/A_i*100 is equal to 11.5% and 13.7% (Figures 12c and 12d), the maximum shear resistance at the feet of the columns of the frame is equal

to 238 kN at 0.75% drift ratio while the maximum shear resistance at the base of the infill wall is equal to 108 kN at 0.25%.

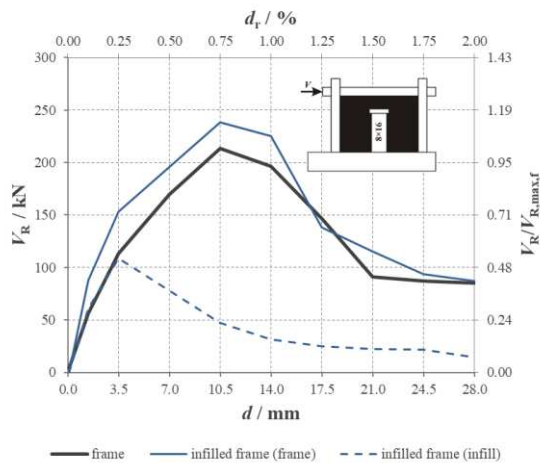
Finally, when the A_o/A_i*100 is equal to 13.5% (Figure 12e), the maximum shear resistance of the columns of the frame is equal to 230 kN at 0.75% drift ratio while the maximum shear resistance of the masonry infill wall is equal to 104 kN at 0.25% drift ratio.



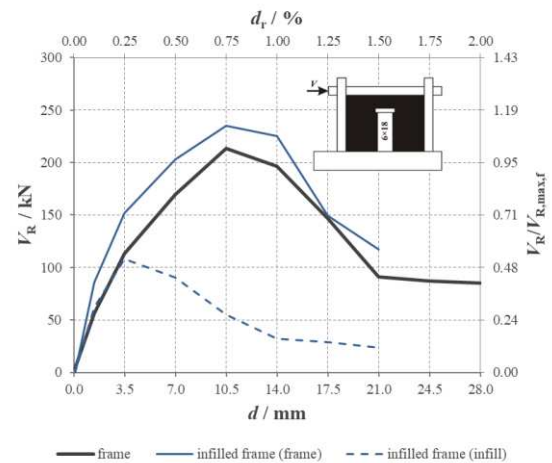
a) $A_o/A_i*100 = 10.3\%$



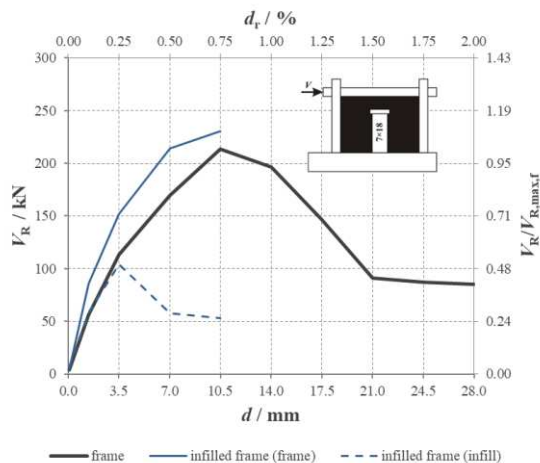
b) $A_o/A_i*100 = 12.3\%$



c) $A_o/A_i*100 = 13.7\%$



d) $A_o/A_i*100 = 11.5\%$

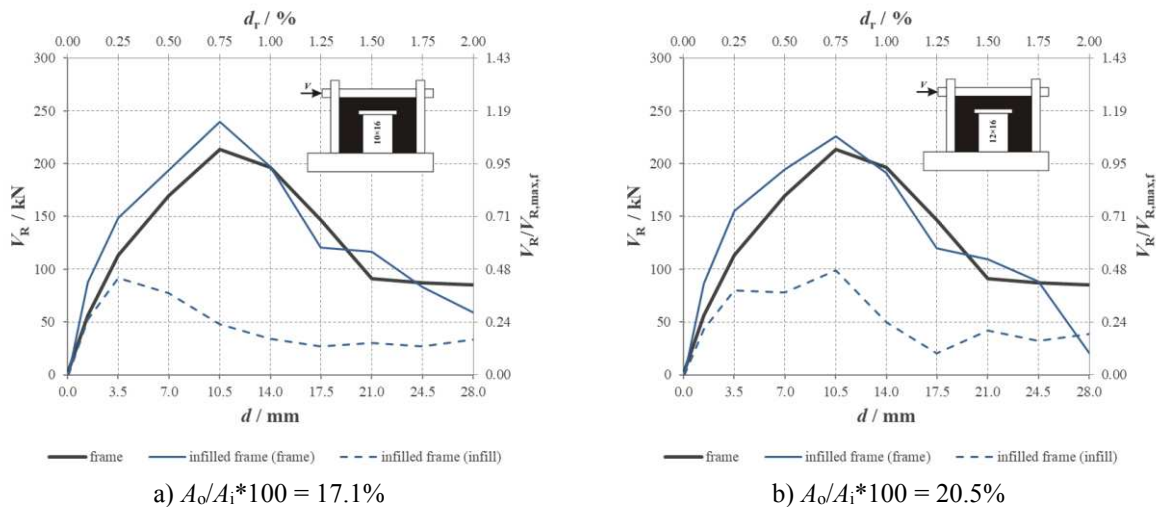


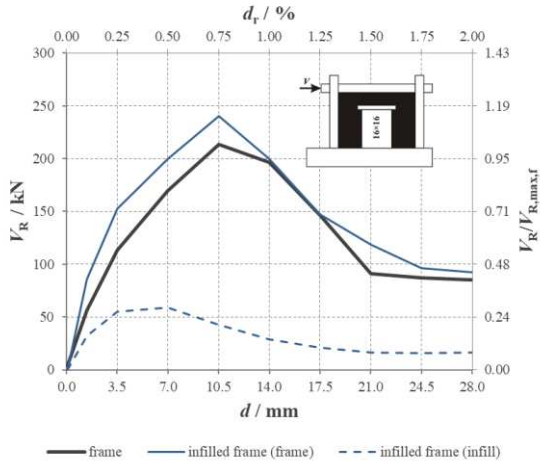
e) $A_o/A_i*100 = 13.5\%$

Figure 12. Shear resistance at the base of the masonry infill wall and at the feet of the reinforced concrete (RC) frame against the drift ratio of masonry infilled RC frames containing a medium size door opening positioned centrally.

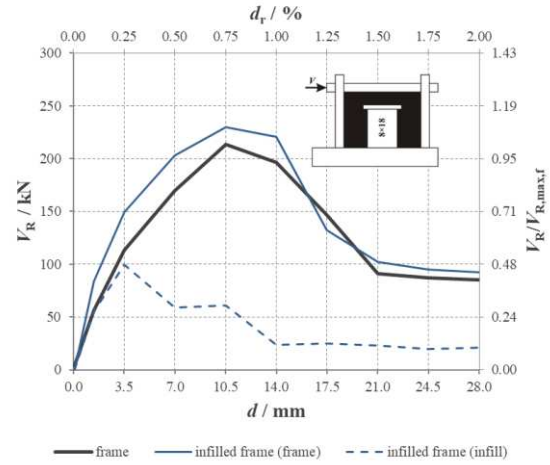
4.2.2 Masonry infill with large size door opening positioned centrally

Figure 13 shows the shear resistance at the base of the masonry infill wall and at the “feet” of the RC frame against the drift ratio of masonry infilled RC frames containing large size door openings positioned centrally. From Figure 13, for the infilled RC frame with large size door openings positioned centrally, the maximum shear resistance at the “feet” of the RC columns increases 7 to 13% when compared with the shear resistance at the “feet” of the RC columns of the bare frame. The maximum shear resistance at the base of the masonry infill wall of the masonry infilled RC frames with large size door openings positioned centrally reduces 50 to 75% when compared with the masonry infill wall without openings. When A_o/A_i*100 ranges between 15.4 and 30.8%, the maximum shear resistance at the “feet” of the RC columns of the frame is almost constant. However, for the same percentage of opening A_o/A_i*100 , the maximum shear resistance of the infill wall reduces almost linearly by 50%.

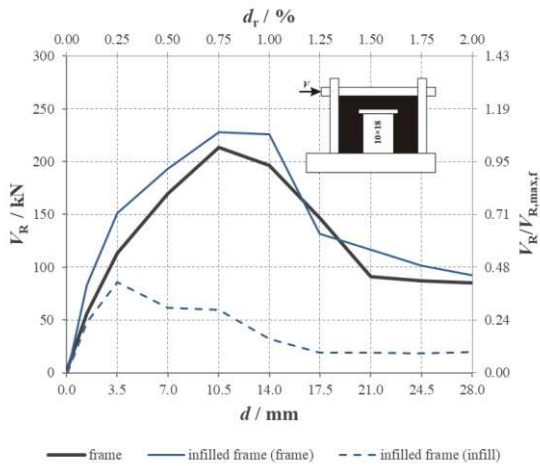




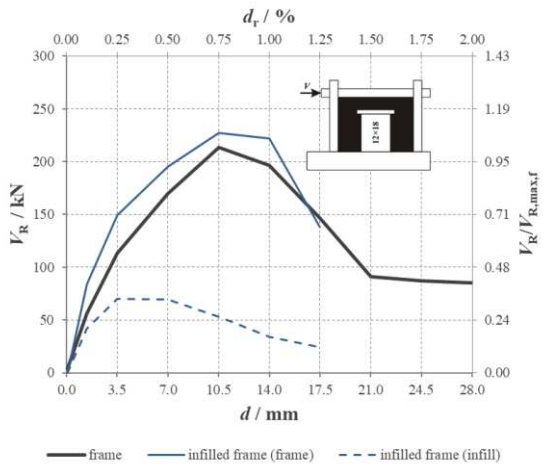
c) $A_o/A_i * 100 = 27.4\%$



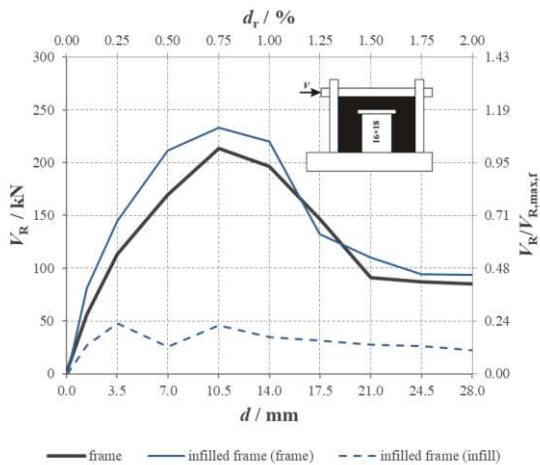
d) $A_o/A_i * 100 = 15.4\%$



e) $A_o/A_i * 100 = 19.2\%$

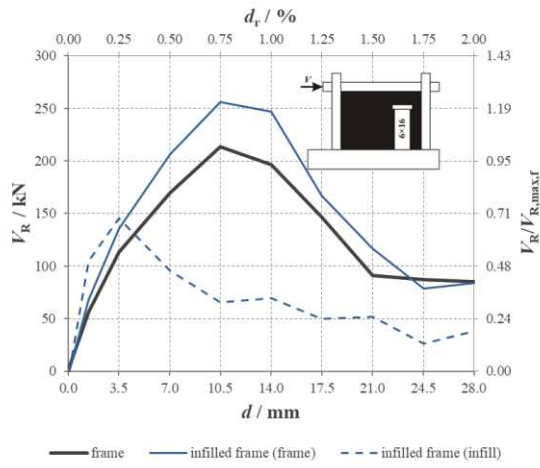


f) $A_o/A_i * 100 = 23.1\%$

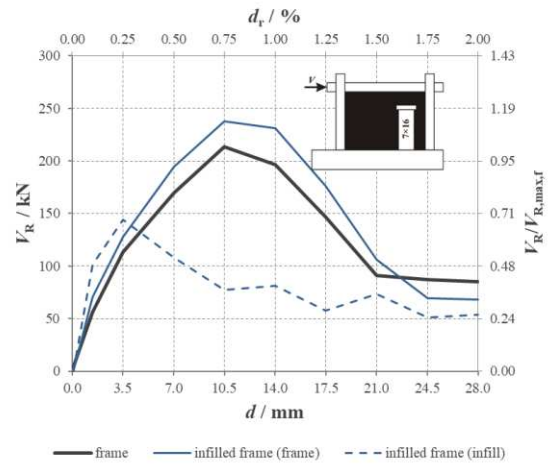


g) $A_o/A_i * 100 = 30.8\%$

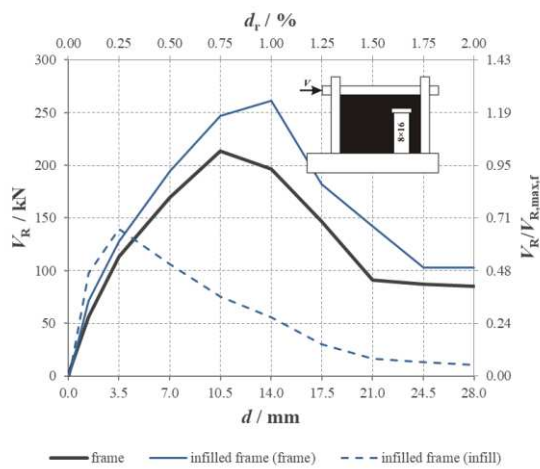
Figure 13. Shear resistance at the base of the masonry infill wall and at the feet of the reinforced concrete (RC) frame against the drift ratio of masonry infilled RC frames containing large size door openings positioned centrally.



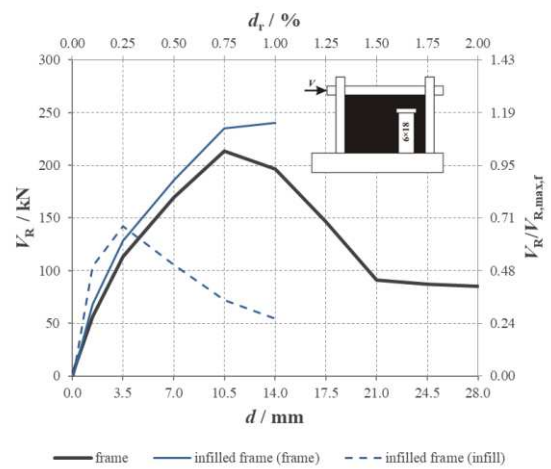
a) $A_o/A_i*100 = 10.3\%$



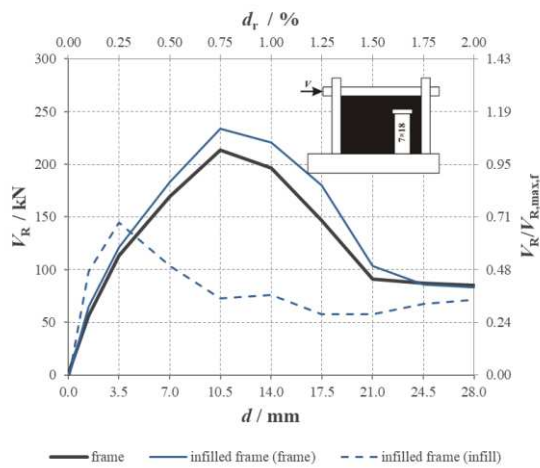
b) $A_o/A_i*100 = 12.3\%$



c) $A_o/A_i*100 = 13.7\%$



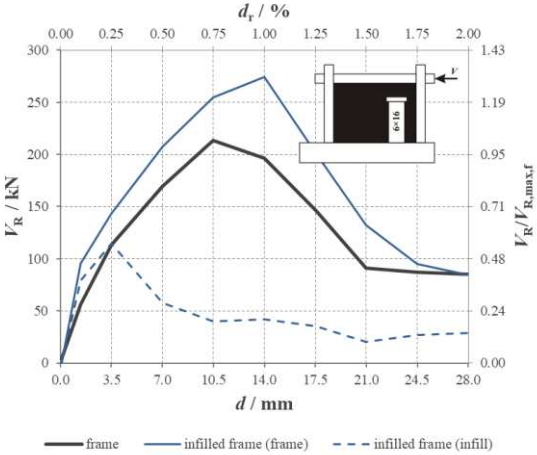
d) $A_o/A_i*100 = 11.5\%$



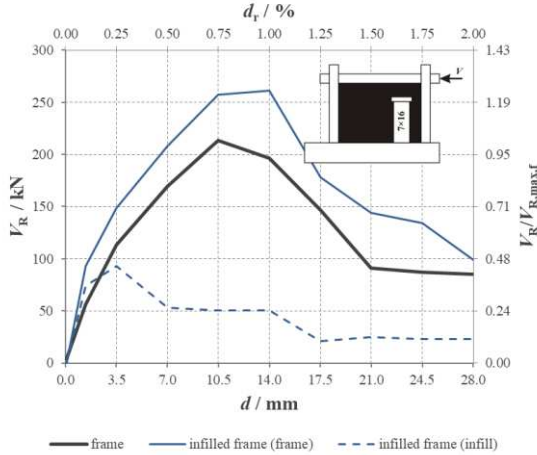
e) $A_o/A_i*100 = 13.5\%$

Figure 16. Shear resistance at the base of the masonry infill wall and at the feet of the reinforced concrete (RC) frame against the drift ratio of masonry infilled RC frames containing medium size door openings positioned eccentrically (load applied from left to right, i.e., positive direction).

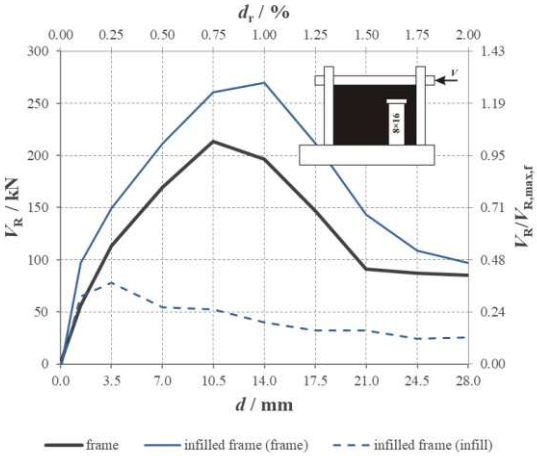
However, the shear resistance at the base of the masonry infill wall of the infilled RC frame is 30% lower than the one of the masonry infill wall without openings. In addition, Figure 17 shows the shear resistance at the base of the masonry infill wall and at the feet of the RC frame against the drift ratio of masonry infilled RC frame containing medium size door openings positioned eccentrically (load applied from right to left, i.e., negative direction).



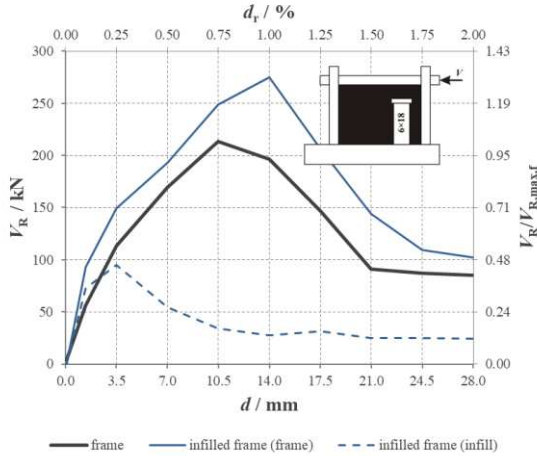
a) $A_0/A_1 \cdot 100 = 10.3\%$



b) $A_0/A_1 \cdot 100 = 12.3\%$



c) $A_0/A_1 \cdot 100 = 13.7\%$



d) $A_0/A_1 \cdot 100 = 11.5\%$

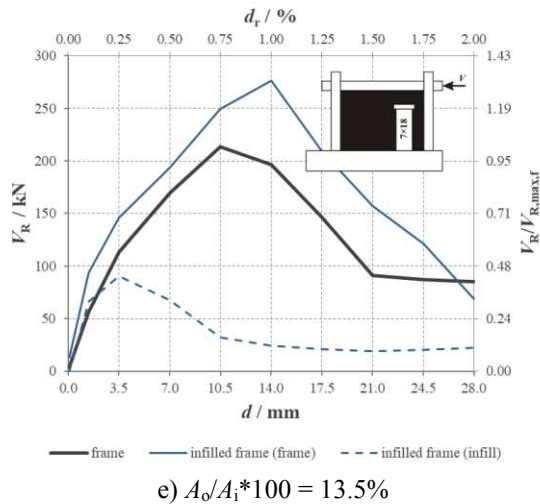
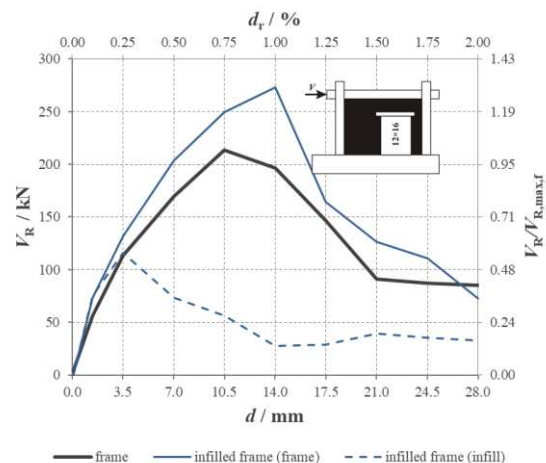
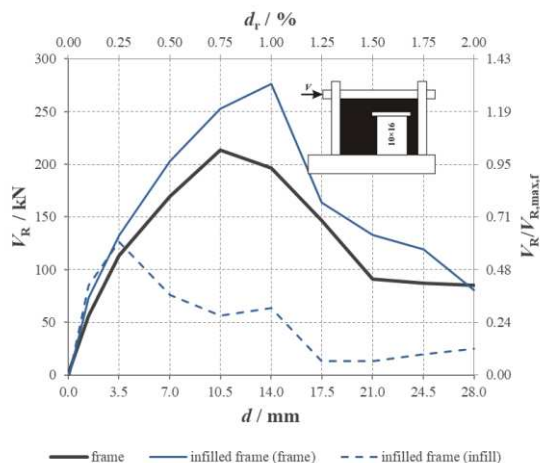


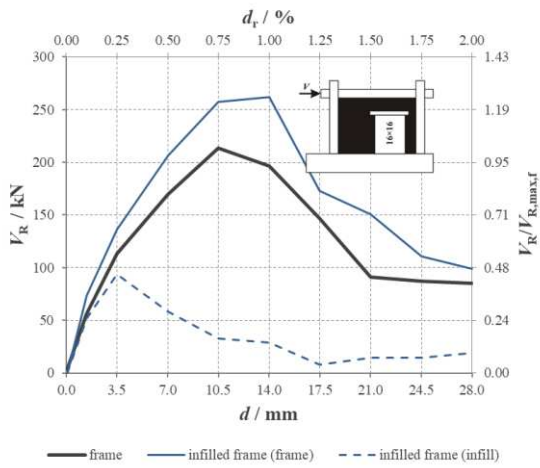
Figure 17. Shear resistance at the base of the masonry infill wall and at the feet of the reinforced concrete (RC) frame against the drift ratio of masonry infilled RC frame containing medium size door openings positioned eccentrically (load applied from right to left, i.e., negative direction).

From Figure 17, the shear resistance at the feet of the columns of the RC frame is 20 to 24% higher than that of RC columns of the bare frame. The shear resistance at the base of the infill wall is also 43 to 63% lower than the one of the masonry infill wall in the infilled RC frame with no openings.

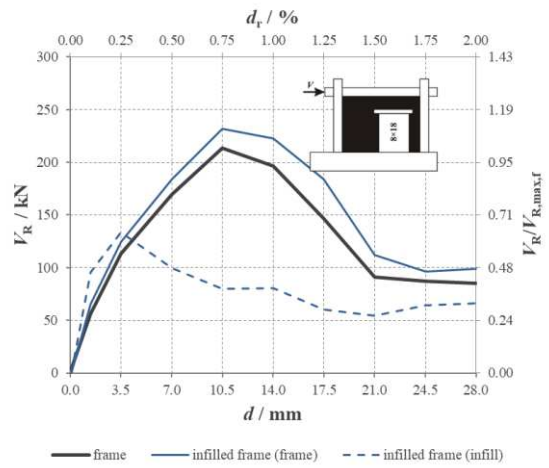
In addition, Figure 18 shows the shear resistance at the base of the masonry infill wall and at the feet of the RC frame against the drift ratio of masonry infilled RC frames containing large size door openings positioned eccentrically (load applied from left to right, i.e., positive direction). In this case, the load was applied on the top left beam end (in the left to right direction). From Figure 18, the shear resistance at the feet of the columns of the masonry infilled RC frame is 33 to 55% higher than that of the bare frame. The shear resistance at the base of the infill wall is also 10 to 23% lower than that of the infill wall without openings.



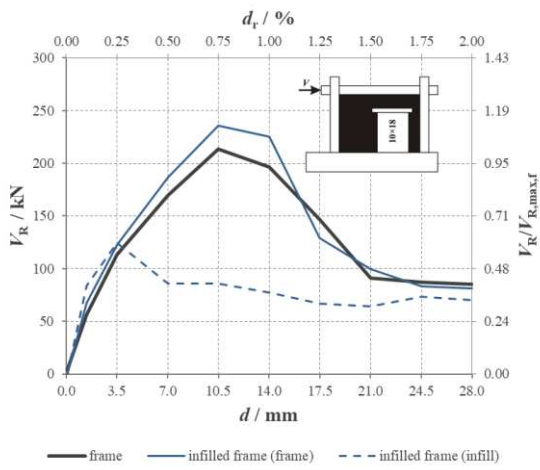
a) $A_0/A_i*100 = 17.1\%$



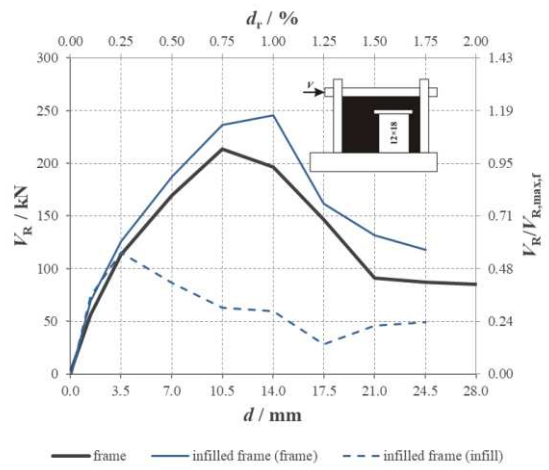
b) $A_0/A_i*100 = 20.5\%$



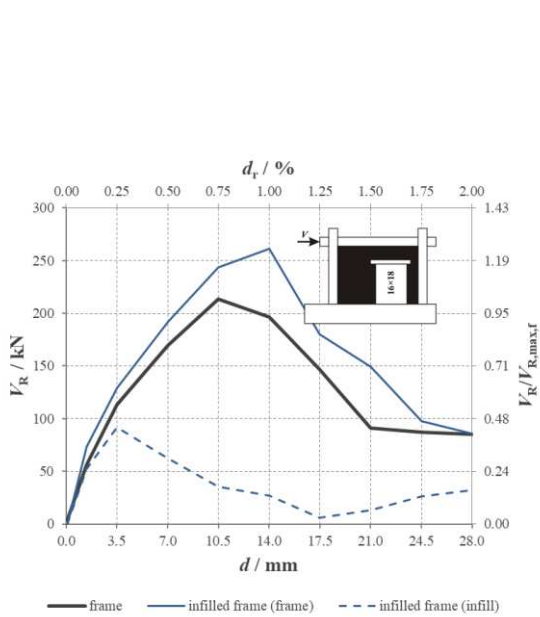
c) $A_0/A_i*100 = 27.4\%$



d) $A_0/A_i*100 = 15.4\%$



e) $A_0/A_i*100 = 19.2\%$



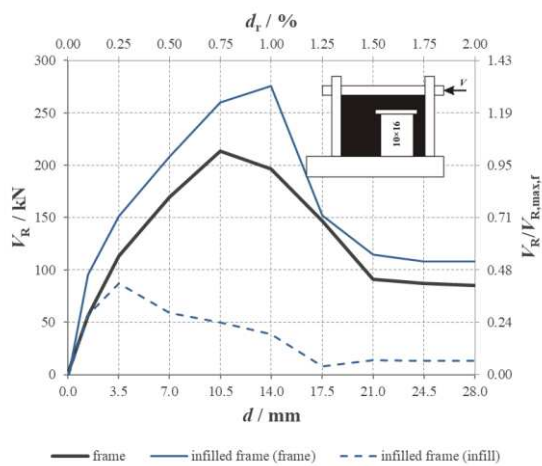
f) $A_0/A_i*100 = 23.1\%$



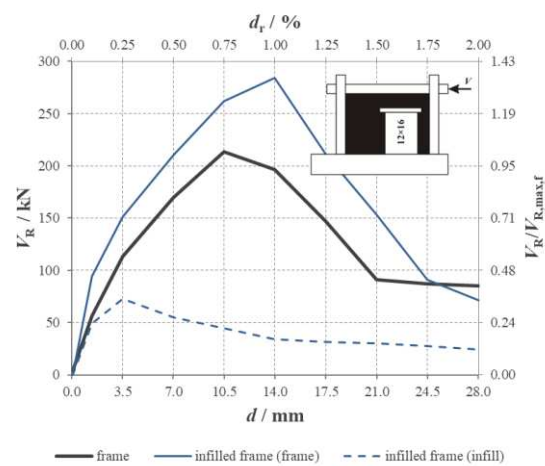
g) $A_0/A_i*100 = 30.8\%$

Figure 18. Shear resistance at the base of the masonry infill wall and at the feet of the reinforced concrete (RC) frame against the drift ratio of masonry infilled RC frames containing large size door openings positioned eccentrically (load applied from left to right, i.e., positive direction).

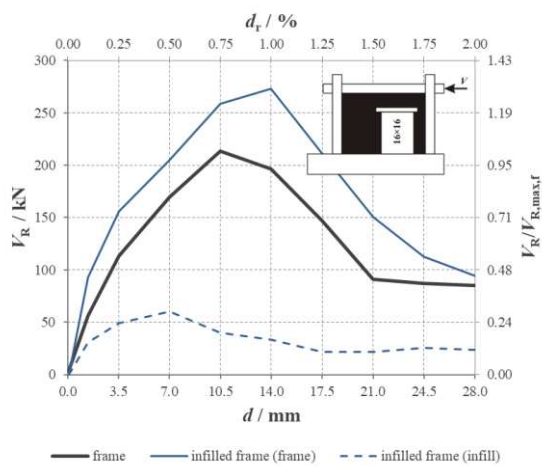
In addition, Figure 19 shows the shear resistance at the base of the masonry infill wall and at the feet of the RC frame against the drift ratio of masonry infilled RC frames containing large size door openings positioned eccentrically (load applied from right to left, i.e., negative direction). In Figure 19, the maximum shear resistance at the feet of the columns of the infilled RC frames is 20 to 26% higher than that of the bare frame. Shear resistance at the base of the masonry infill wall is also 53 to 70% lower than that of the masonry infill wall without openings.



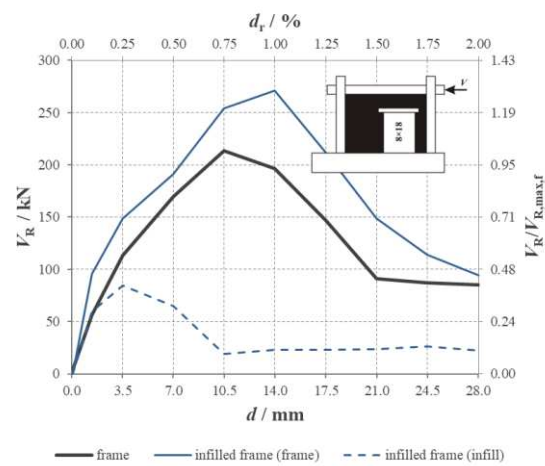
a) $A_0/A_1 \cdot 100 = 17.1\%$



b) $A_0/A_1 \cdot 100 = 20.5\%$



c) $A_0/A_1 \cdot 100 = 27.4\%$



d) $A_0/A_1 \cdot 100 = 15.4\%$

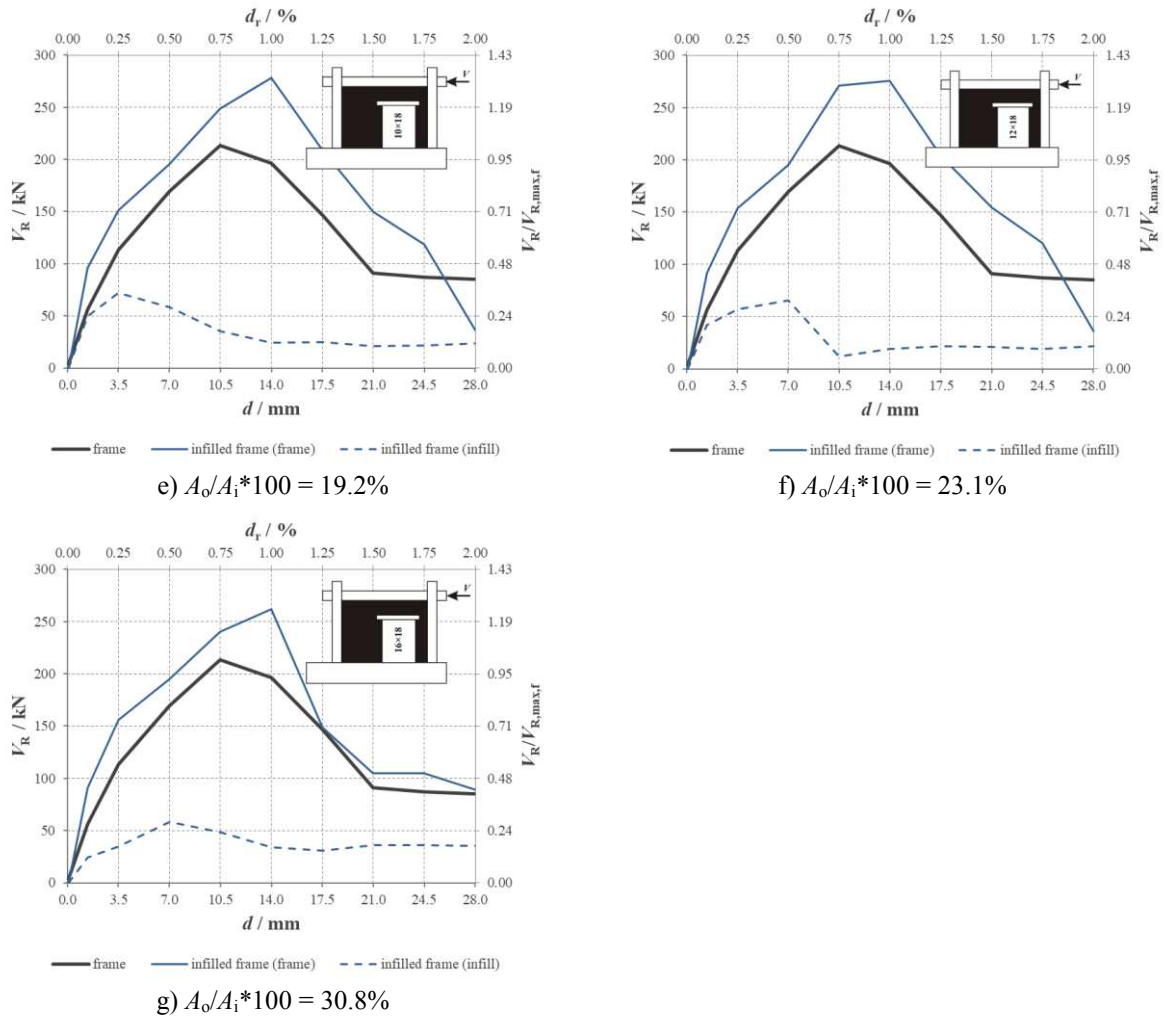


Figure 19. Shear resistance at the base of the masonry infill wall and at the feet of the reinforced concrete (RC) frame against the drift ratio of masonry infilled RC frames containing large size door openings positioned eccentrically (load applied from right to left, i.e., negative direction).

4.4.2 Masonry infill with window openings positioned eccentrically

Figure 20 shows the shear resistance at the base of the masonry infill wall and at the feet of the RC frame against the drift ratio of masonry infilled RC frames containing medium size window openings positioned eccentrically. In Figures 20a and 20b, and when the load is applied from left to right (i.e., positive direction), the shear resistance at the feet of the RC columns of the frames is 25% higher than that of the bare frame. The shear resistance of the masonry infill wall is also 8 to 19% lower than that of the infill wall without openings. In Figures 20c and 20d, and when the load is applied from right to left (i.e., negative direction), the maximum shear resistance at the feet of the RC columns of the masonry infilled frame is 15 to 18% higher than that of the bare frame. The shear resistance at the base

of the masonry infill wall of the masonry infilled RC frame with eccentrically positioned openings (negative direction) is also 34 to 37% lower than that of the masonry infill wall without openings.

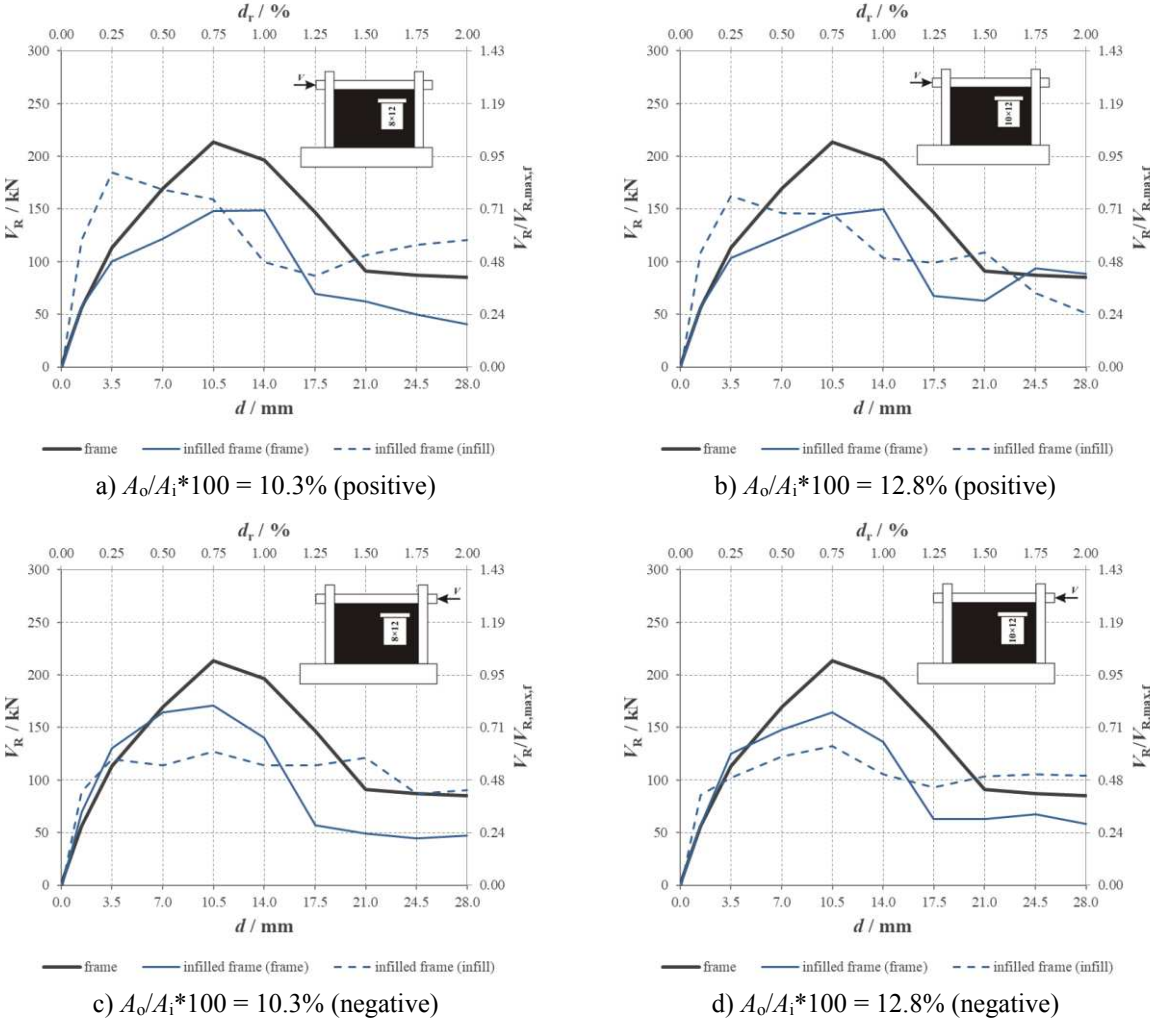


Figure 20. Shear resistance at the base of the masonry infill wall and at the feet of the reinforced concrete (RC) frame against the drift ratio of masonry infilled RC frames containing medium size window openings positioned eccentrically.

Figure 21 shows the shear resistance at the base of the masonry infill wall and at the feet of the RC frame against the drift ratio of masonry infilled RC frames containing large size window openings positioned eccentrically. From Figures 21a and 21b, when the load is applied from right to left (i.e., negative direction), the maximum shear resistance of the columns of the frame is 29 to 32% higher than that of the bare frame. The shear resistance at the base of the infill wall is also 21 to 24% lower than that of the infill wall without openings. On the other hand, in Figures 21c and 21d, when the load is applied from right to left (i.e., negative direction), the shear resistance at the feet of the RC columns of the infilled frame is 15% higher than that of the bare frame. The shear resistance of the masonry infill wall is also 42 to 43% lower than the one of the masonry infill wall without openings.

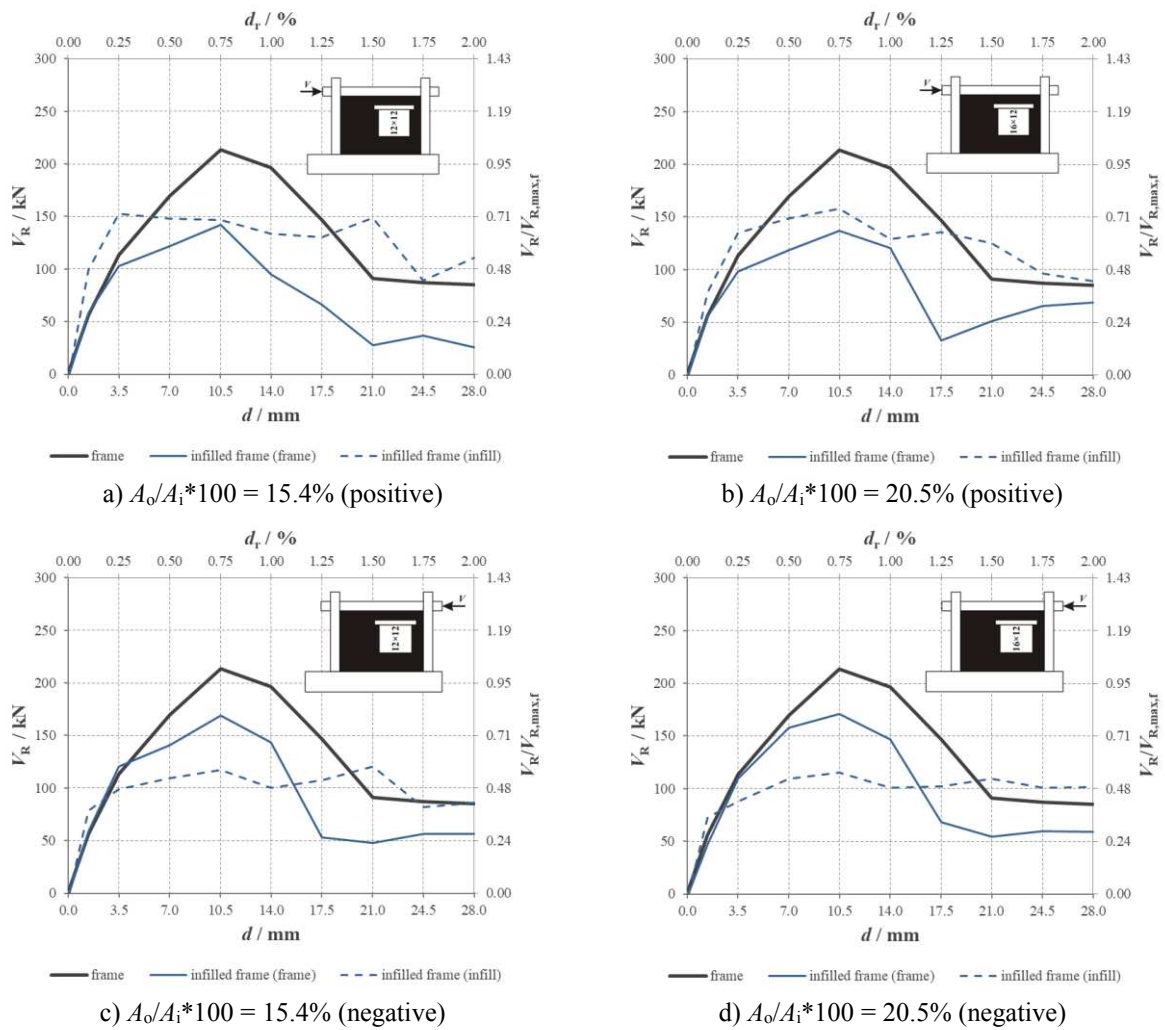


Figure 21. Shear resistance at the base of the masonry infill wall and at the feet of the reinforced concrete (RC) frame against the drift ratio of masonry infilled RC frames containing large size window openings positioned eccentrically.

4.4.3 Variation of shear resistance in infilled masonry containing different size and location of openings

Figure 22 shows the normalized shear resistance of infilled RC frames with door openings with respect to the bare RC frame against the ratio of the area of the opening to the area of the masonry infill wall. In Figure 22, the actual shear resistance of the RC frame is not influenced by the opening size, type and position. For infilled frames with centrally positioned door openings, the actual shear resistance is 10% of that of the bare frame, while for eccentrically positioned door openings, the actual resistance is 23%. In addition, for infilled RC frames with door openings, the shear resistance of the frame decreases almost linearly by 30% as the ratio of the area of opening to the area of the infill

(A_o/A_i) increases from 10.3 to 30.8%. For masonry infilled RC frames with eccentrically positioned door openings (and the load applied in the positive direction, i.e., from left to right), the shear resistance of the frame increases by 20% when compared with the shear resistance of the masonry infilled RC frame with door openings positioned centrally and the masonry infilled RC frame with door openings positioned eccentrically (load applied in the negative direction, i.e., from right to left). By extrapolating the trendline of the shear resistance in Figure 22, the shear resistance of masonry infill wall compared with the shear resistance of the bare frame is about 15% at $A_o/A_i \cdot 100 = 35\%$ (a limit value for differentiation between primary and secondary members of the system in compliance with EN 1998-1 (CEN 2004b)).

Figure 23 shows the normalized shear resistance of infilled RC frames with window openings with respect to the bare RC frame against the ratio of the area of the opening to the area of the masonry infill wall. For infilled RC frames with window openings positioned eccentrically (negative), the normalized shear resistance of the RC frame is not affected by the size of the opening. However, for infilled RC frames with window openings positioned eccentrically (negative), the normalized shear resistance of the masonry infill frame reduces by 10% as the area of opening to the area of the infill (A_o/A_i) increases from 10.3 to 20.5%. In addition, Figure 23b shows the normalized shear resistance of infilled RC frames with windows positioned centrally. For infilled RC frames with window openings positioned centrally, the normalized shear resistance of the RC frame is not affected by the size of the opening. However, for infilled RC frames with window openings positioned centrally, the normalized shear resistance of the masonry infill frame reduces by 25% as the area of opening to the area of the infill (A_o/A_i) increases from 10.3 to 20.5%. Figure 23c shows the normalized shear resistance of infilled RC frames with eccentrically positioned windows. For infilled RC frames with window openings positioned eccentrically (positive), the normalized shear resistance of the RC frame is not affected by the size of the opening. However, for infilled RC frames with window openings positioned eccentrically (negative), the normalized shear resistance of the masonry infill frame reduces by 15% as the area of opening to the area of the infill (A_o/A_i) increases from 10.3 to 20.5%.

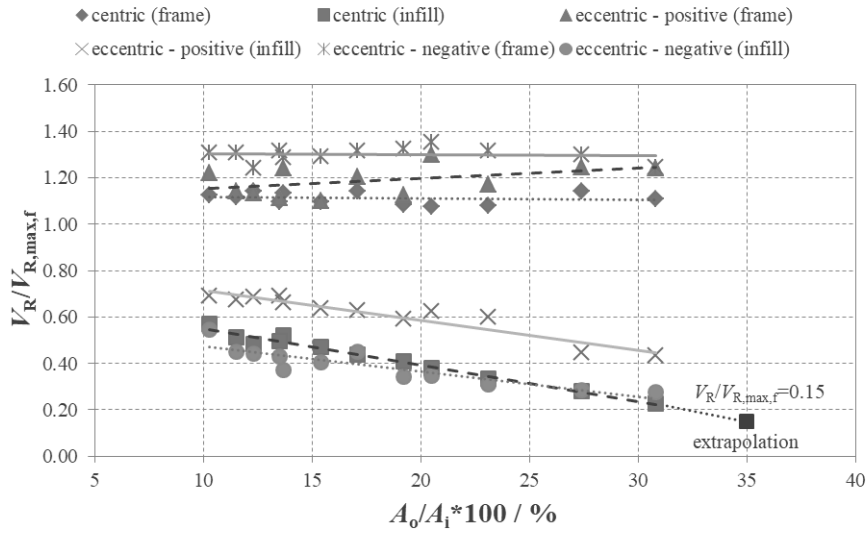
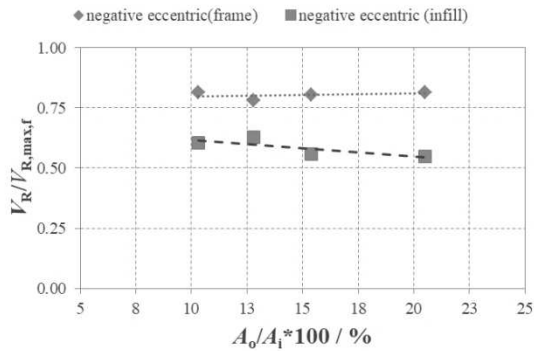
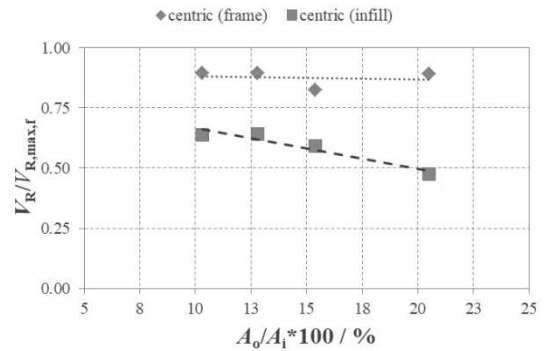


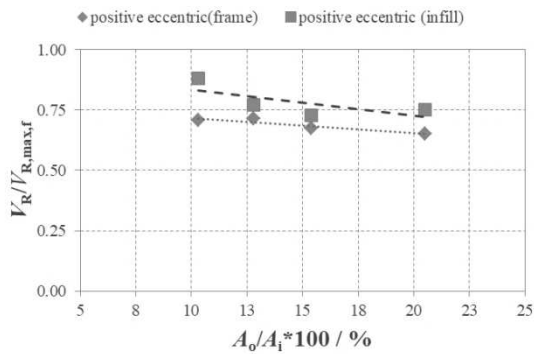
Figure 22. Shear resistance ($V_R/V_{R,f}$) of reinforced concrete frames with masonry infill walls with door openings against ratio of opening area to masonry infill wall area (A_o/A_i*100).



a) Eccentrically positioned window opening (negative)



b) Centrally positioned window opening

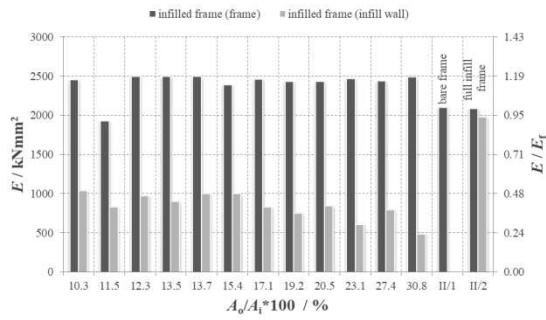


c) Eccentrically positioned window opening (positive)

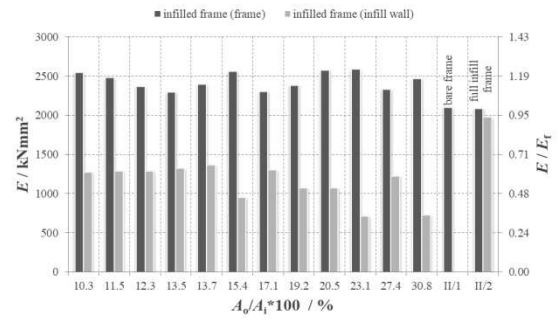
Figure 23. Shear resistance ($V_R/V_{R,f}$) of reinforced concrete frames with masonry infill walls with window openings against ratio of opening area to masonry infill wall area (A_o/A_i*100).

4.4.4 Deformation capacity

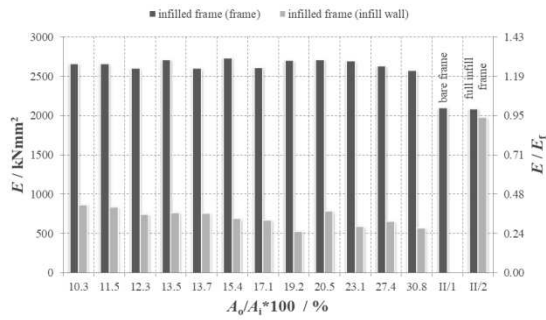
The deformation capacity (E) or the area beneath the curves of the Figures 19 to 21 up to a drift ratio equal to 1% was estimated and is shown in Figure 24. For the masonry infilled RC frames containing door openings, the deformation capacity of the RC columns of the infilled frame is higher than that of the columns of the bare frame. In Figure 24 it is observed that the deformation capacity demand of the masonry infilled wall and that of the RC frame for the infilled RC frame with no opening is almost the same. For masonry infilled RC frames with door openings positioned eccentrically (negative), the deformation capacity of the RC frame is higher than masonry infilled RC frames with door opening positioned centrally or eccentrically (when the load applied in the positive direction, i.e., from left to right). However, for masonry infilled RC frames with door openings positioned eccentrically (negative), the deformation capacity of the masonry infill wall is lower than that of the masonry infilled RC frames with door opening positioned centrally or eccentrically (when the load is applied in the positive direction, i.e., from left to right). It should also be noted that in the case where the area of the opening to the area of the masonry infill is equal to 11.5% for masonry infilled RC frames with door openings centrally positioned the drift ratio was 0.75% and that is why the resistance deformation capacity is lower than that of the other cases. This was due to loss of stability in the masonry pier due to the development of a diagonal crack that originated from two thirds of the height of the wall to the left-hand bottom corner of the door opening. Similar results were also obtained in the experiment (Figure E, specimen I/1). In addition, from Figures 24a to 24c, and for the infilled RC frames containing door openings, the deformation capacity of the masonry infill wall is higher than that of the RC frame. Similarly, from Figure 24d, for infilled RC frames containing centrally positioned window openings, the deformation capacity of the masonry infill wall is higher than that of the RC frame. For the infilled RC frames containing eccentrically positioned window openings, the deformation capacity of the masonry infill wall is lower than that of the reinforced concrete frame. This is due to the failure mechanism which developed in the masonry infill wall. For centrally positioned window openings, the failure mechanism is due to a diagonal tensile failure of the masonry pier (Figure E, spec I/2). In this case the deformation capacity of the masonry infill wall was higher than that of the RC frame. However, the failure mechanism of the eccentrically positioned window openings is due to bed joint sliding of the masonry pier (Figure E, spec I/4). Moreover, from Figures 24b and 24c, for the infilled RC frames with door openings positioned eccentrically and the load applied from the left to right direction, the deformation capacity of the masonry infill wall is lower than those applied from the right to left direction. This is because the diagonal stress path is interrupted by the presence of the opening (see Figure 25).



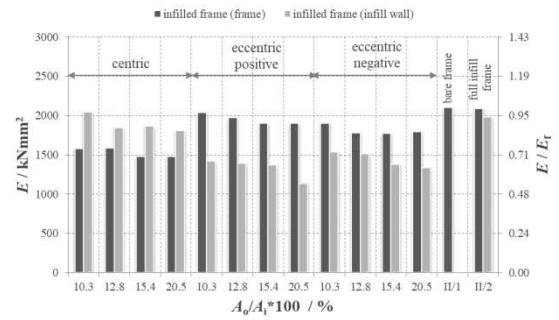
a) Door openings centrally positioned



b) Door openings eccentrically positioned (positive)



c) Door openings eccentrically positioned (negative)



d) Window openings

Figure 24. Deformation capacity (E) against the area of opening to area of infill ratio (A_o/A_i).

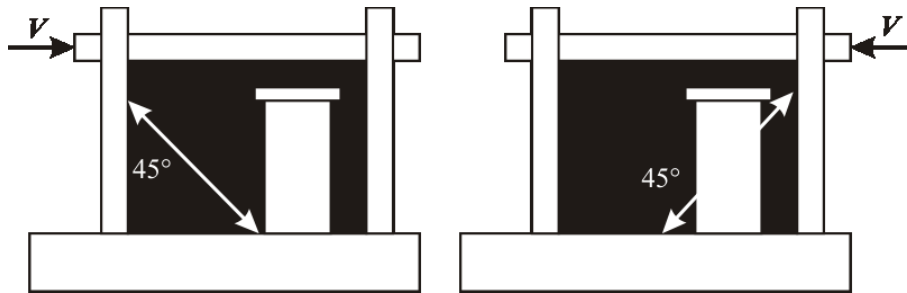


Figure 25. Interruption of the diagonal path in the case of an eccentrically positioned opening.

5 Conclusions

This paper investigates the influence of the opening type, size and position on the shear resistance and deformation capacity of the individual components (e.g., the masonry infilled wall and reinforced concrete frame columns) of masonry infilled RC frame structures. A computational model based on the non-linear FE method of analysis has been developed. The computational model has been validated against a series of experimental tests carried out in the laboratory. An extensive parametric study was carried out to investigate the influence of opening size (e.g., windows and doors) on the lateral stiffness of the masonry infilled RC frame structures. The internal shear forces in the masonry infill wall and RC frame columns of the framed-wall system at various damage grades were computed

and compared with the corresponding shear forces of the bare frame. From the results analysis, and for this particular geometry of the infilled RC frame, it was found that:

- The shear resistance of the individual components (e.g., masonry infill wall without openings, and RC frame) is almost the same as the shear resistance of the bare RC frame.
- The shear resistance of masonry infill wall components is influenced by the size, location and type of opening. The shear resistance of the structural components of the masonry infill decreases as the ratio of the area of the opening to the area of the masonry infill wall increases.
- The shear resistance at the columns of the infilled RC frame with window and door openings is not related to the opening type, size and position.
- For masonry infilled RC frames with centrally positioned window openings and eccentrically positioned window openings (negative), the RC frame carries more shear resistance than the masonry infill wall.
- For masonry infilled RC frames with eccentrically positioned window openings (positive), the RC frame carries less shear resistance than the masonry infill wall.
- The contribution of the shear resistance of the frame in infilled frames containing door openings exceeds the shear resistance of the bare frame. For the case of infilled frames containing eccentrically positioned door openings the shear resistance is higher than that of the infilled frames containing centrally positioned door openings.
- For infilled RC frames with window openings positioned centrally, the deformation capacity of the masonry infill wall is higher than the deformation capacity of the RC frame and lower compared with the bare frame and the fully infilled frame.
- However, for infilled RC frames with window openings positioned eccentrically, the deformation capacity of the masonry infill frame is higher than that of the RC frame and lower compared with the bare frame and the fully infilled frame.
- The deformation capacity of the frame is significantly higher than the deformation capacity of the masonry infill wall and that of the bare RC frame.
- For the masonry infill wall with door openings, the deformation capacity is significantly lower than the deformation capacity of the bare RC frame. The contribution of their significance is in the following order: a) infill walls with door openings eccentricity positioned (positive); b) infill walls with centrally position door openings; and c) infill walls with door openings eccentricity positioned (negative).

In conclusion, the size, location and type of opening do influence the design characteristics of the infilled RC frame. In particular, the shear resistance at columns of the infilled RC frame with door opening is higher by the shear resistance of the columns of the RC frame. In design, the contribution

of the shear capacity of the frame is underestimated and this can lead to inaccurate predictions of the system's response. However, the shear resistance at columns of the infilled RC frame with window opening is lower than the shear resistance of the columns of the RC frame. In design, the contribution of the shear capacity of the frame is overestimated.

In the future, parametric studies on masonry infilled reinforced concrete frames with different geometries will be carried out. The influence of door and window opening of different sizes and positions in the same masonry infill wall on the shear resistance of the individual components of the infilled RC frame will be investigated.

Acknowledgements

The research presented in this article is a part of the research project *FRamed-Masonry composites for modelling and standardization (HRZZ-IP-2013-11-3013)* supported by Croatian Science Foundation and its support is gratefully acknowledged. The authors are grateful to Professor Vladimir Sigmund (1956–2016) for his significant contribution to and direction of the research undertaken in this paper.

References

- Achyutha, H. et al., 1986. Finite element simulation of the elastic behaviour of infilled frames with openings. *Computers & Structures*, 23(5), pp.685–696. Available at: <http://linkinghub.elsevier.com/retrieve/pii/0045794986900775> [Accessed July 28, 2017].
- Al-Chaar, G.K., Lamb, G.E. & Issa, M.A., 2003. Effect of openings on structural performance of unreinforced masonry infilled frames. *ACI Special Publication*, 211, pp.247–262.
- Anić, F., Penava, D. & Sarhosis, V., 2017. Development of a three-dimensional computational model for the in-plane and out-of-plane analysis of masonry-infilled reinforced concrete frames. In M. Papadrakakis & M. Fragiadakis, eds. *COMPADYN 2017 6th ECCOMAS Thematic Conference on Computational Methods in Structural Dynamics and Earthquake Engineering*. Rhodes Island, Greece, pp.1–15.
- Asteris, P.G. et al., 2016. A macro-modelling approach for the analysis of infilled frame structures considering the effects of openings and vertical loads. *Structure and Infrastructure Engineering*, 12(5), pp.551–566.
- Asteris, P.G., 2003. Lateral stiffness of brick masonry infilled plane frames. *ASCE Journal of Structural Engineering*, 129(8), pp.1071–1079.
- Asteris, P.G. et al., 2011. Mathematical macromodeling of infilled frames: state of the art. *Journal of Structural Engineering*, 137(12), pp.1508–1517.
- Asteris, P.G. et al., 2013. Mathematical micromodeling of infilled frames: state of the art. *Engineering Structures*, 56, pp.1905–1921.

- Asteris, P.G. et al., 2015. On the fundamental period of infilled RC frame buildings. *Structural Engineering and Mechanics*, 54(6), pp.1175–1200.
- Asteris, P.G., Ioannis, P.G. & Chrysostomou, C.Z., 2012. Modeling of infilled frames with openings. *The Open Construction and Building Technology Journal*, 6, pp.81–91.
- Bažant, Z.P. & Chern, J.C., 1985. Strain softening with creep and exponential algorithm. *Journal of Engineering Mechanics*, 111(3), pp.391–415.
- Bažant, Z.P. & Oh, B.H., 1983a. Crack band theory for fracture of concrete. *Matériaux et Constructions*, 16(3), pp.155–177. Available at: <http://link.springer.com/10.1007/BF02486267> [Accessed May 4, 2015].
- Bažant, Z.P. & Oh, B.H., 1983b. Spacing of cracks in reinforced concrete. *Journal of Structural Engineering*, 109(9), pp.2066–2085. Available at: <http://ascelibrary.org/doi/abs/10.1061/%28ASCE%290733-9445%281983%29109%3A9%282066%29> [Accessed May 4, 2015].
- Bažant, Z.P. & Planas, J., 1997. *Fracture and size effect in concrete and other quasibrittle materials*, CRC Press.
- Benjamin, J.R. & Williams, H.A., 1958. The behavior of one-story brick shear walls. *Journal of the Structural Engineering Division, Proceedings of the American Society of Civil Engineers*, 84, pp.1–30.
- Cavaleri, L. et al., 2017. Influence of column shear failure on pushover based assessment of masonry infilled reinforced concrete framed structures: A case study. *Soil Dynamics and Earthquake Engineering*, 100, pp.98–112. Available at: <http://linkinghub.elsevier.com/retrieve/pii/S0267726116304924> [Accessed July 28, 2017].
- Cavaleri, L. & Di Trapani, F., 2014. Prediction of the additional shear action on frame members due to infills. *Bulletin of Earthquake Engineering*, 13(5), pp.1425–1454. Available at: <http://link.springer.com/10.1007/s10518-014-9668-z> [Accessed May 20, 2015].
- CEN, 2004a. *Eurocode 2: Design of concrete structures - Part 1-1: General rules and rules for buildings (EN 1992-1-1:2004)*, Brussels: European Committee for Standardization.
- CEN, 2005. *Eurocode 6: Design of masonry structures - Part 1-1: General rules for reinforced and unreinforced masonry structures (EN 1996-1-1:2005)*, Brussels: European Committee for Standardization.
- CEN, 2004b. *Eurocode 8: Design of Structures for Earthquake Resistance - Part 1: General Rules, Seismic Actions and Rules for Buildings (EN 1998-1:2004)*, Brussels: European Committee for Standardization.
- CEN, 2009. *Testing hardened concrete – Part 3: Compressive strength of test specimens (EN 12390-3:2009)*, Brussels: European Committee for Standardization.
- Cervenka, V., Jendele, L. & Cervenka, J., 2012. *ATENA Program Documentation Part 1 Theory*, Prague: Cervenka Consulting Ltd.

- Cervenka Consulting s.r.o., 2015. *ATENA for Non-Linear Finite Element Analysis of Reinforced Concrete Structures*. Prague: Cervenka Consulting Ltd.
- Crisafulli, F.J. & Carr, A.J., 2007. Proposed Macro-Model for the Analysis of Infilled Frame Structures. *Bulletin of the New Zealand Society for Earthquake Engineering*, 40(2), pp.69–77.
- Crisafulli, F.J., Carr, A.J. & Park, R., 2000. Analytical modelling of infilled frame structures - a general review. *Bulletin of the New Zealand Society for Earthquake Engineering*, 33(1), pp.30–47.
- Crisafulli, F.J., Carr, A.J. & Park, R., 2005. Experimental response of framed masonry structures designed with new reinforcing details. *The New Zealand Society for Earthquake Engineering*, 38(1), pp.1–14.
- El Dakhkhni, W.W., Elgaaly, M. & Hamid, A.A., 2003. Three-strut model for concrete masonry infilled steel frames. *ASCE Journal of Structural Engineering*, 129(2), pp.177–185.
- Dawe, J.L. & Young, T.C., 1985. An investigation of factors influencing the behavior of masonry infill in steel frames subjected to in-plane shear. In *Proceedings of the 7th International Brick and Block Masonry Conference*. pp.803–814.
- Decanini, L.D., Liberatore, L. & Mollaioli, F., 2014. Strength and stiffness reduction factors for infilled frames with openings. *Earthquake Engineering and Engineering Vibration*, 13(3), pp.437–454. Available at: <http://link.springer.com/10.1007/s11803-014-0254-9> [Accessed July 28, 2017].
- Dolšek, M. & Fajfar, P., 2008. The effect of masonry infills on the seismic response of a four-storey reinforced concrete frame — a deterministic assessment. *Engineering Structures*, 30(7), pp.1991–2001.
- Fiorato, A.E., Sozen, M.A. & Gamble, W.L., 1970. *An investigation of the interaction of reinforced concrete frames with masonry filled walls*, Urbana, Illinois.
- Focardi, F. & Manzini, E., 1984. Diagonal tension tests on reinforced and non-reinforced brick panels. In *Proceedings of the 8th World Conference on Earthquake Engineering*. San Francisco, California, pp. 839–846.
- Gazić, G. & Sigmund, V., 2013. Experimental investigation of weak R/C frames with masonry infill. In *International Conference on Earthquake Engineering (SE-50EEE) “50 years Skopje earthquake - 50 years European earthquake engineering.”* Skoplje, Makedonija.
- Grünthal, G. et al., 1998. *European macroseismic scale 1998*, Luxembourg.
- Kakaletsis, D.J. & Karayannis, C.G., 2007. Experimental investigation of infilled R/C frames with eccentric openings. *Structural Engineering and Mechanics Journal*, 26(231–250).
- Kakaletsis, D.J. & Karayannis, C.G., 2009. Experimental investigation of infilled reinforced concrete frames with openings. *ACI Structural Journal*, 106(2), pp.132–141.
- Kakaletsis, D.J. & Karayannis, C.G., 2008. Influence of masonry strength and openings on infilled R/C frames under cycling loading. *Journal of Earthquake Engineering*, 12(2), pp.197–221.

- Koutromanos, I. et al., 2011. Numerical modeling of masonry-infilled RC frames subjected to seismic loads. *Computers and Structures*, 89(11–12), pp.1026–1037. Available at: <http://dx.doi.org/10.1016/j.compstruc.2011.01.006>.
- Koutromanos, I. & Shing, P.B., 2012. Cohesive crack model to simulate cyclic response of concrete and masonry structures. *ACI Structural Journal*, 109(3), pp.349–358.
- Liauw, T.C. & Kwan, K.H., 1985. Static and cyclic behaviours of multistorey infilled frames with different interface conditions. *Journal of Sound and Vibration*, 99(2), pp.275–283. Available at: <http://linkinghub.elsevier.com/retrieve/pii/0022460X85903633> [Accessed July 27, 2017].
- Liu, M., Cheng, Y. & Liu, X., 2011. Shaking table test on out-of-plane stability of infill masonry wall. *Transactions of Tianjin University*, 17(2), pp.125–131. Available at: <http://link.springer.com/10.1007/s12209-011-1534-3> [Accessed September 24, 2015].
- Mainstone, R.J., 1971. On the stiffness and strengths of infilled frames. In *Proceedings of the Institution of Civil Engineers, Supplement (iv)*. pp.57–90.
- Mainstone, R.J., 1974. *Supplementary note on the stiffness and strength of infilled frames*, U. K.
- Mehrabi, A.B. & Shing, P.B., 1997. Finite element modeling of masonry-infilled RC frames. *Journal of Structural Engineering*, 123(5), pp.604–613.
- Moghadam, H.A., 2004. Lateral load behavior of masonry infilled steel frames with repair and retrofit. *ASCE Journal of Structural Engineering*, 130(1), pp.56–63.
- Moghadam, H.A., Mohammadi, M.G. & Ghaemian, M., 2006. Experimental and analytical investigation into crack strength determination of infilled steel frames. *Journal of Constructional Steel Research*, 62(12), pp.1341–1352. Available at: <http://linkinghub.elsevier.com/retrieve/pii/S0143974X06000149> [Accessed July 27, 2017].
- Mohebkhah, A. & Tasnimi, A.A., 2007. Seismic behavior of brick masonry walls recommended by IS-2800: experimental and numerical approaches. In *Proceedings of the 5th Conf. on Seismology and Earthquake Engineering, International Institute of Earthquake Engineering and Seismology*. Tehran, Iran.
- Mohebkhah, A., Tasnimi, A.A. & Moghadam, H.A., 2008. Nonlinear analysis of masonry-infilled steel frames with openings using discrete element method. *Journal of Constructional Steel Research*, 64(12), pp.1463–1472. Available at: <http://linkinghub.elsevier.com/retrieve/pii/S0143974X08000151> [Accessed July 28, 2017].
- Negro, P. & Colombo, A., 1997. Irregularities induced by nonstructural masonry panels in framed buildings. *Engineering Structures*, 19(7), pp.576–585. Available at: <http://linkinghub.elsevier.com/retrieve/pii/S0141029696001150> [Accessed July 28, 2017].
- Neufert, E. & Neufert, P., 2012. *Architects' data* 4th ed., Wiley-Blackwell.
- Papia, M., Cavaleri, L. & Fossetti, M., 2003. Infilled frames: developments in the evaluation of the stiffening effect of infills. *Structural Engineering and Mechanics*, 16(6), pp.675–693. Available at: <http://koreascience.or.kr/journal/view.jsp?kj=KJKHB9&py=2003&vnc=v16n6&sp=675>

- [Accessed July 28, 2017].
- Paulay, T. & Priestley, M.J.N., 1992. *Seismic design of reinforced concrete and masonry buildings*, Wiley.
- Penava, D. et al., 2016. Clay block masonry and mortar joint interlocking. *Journal of the Croatian Association of Civil Engineers*, 68(8), pp.609–616.
- Penava, D., 2012. *Influence of openings on seismic response of masonry infilled reinforced concrete frames*. Josip Juraj Strossmayer University of Osijek, Osijek, Croatia.
- Penava, D., Sigmund, V. & Kožar, I., 2016. Validation of a simplified micromodel for analysis of infilled RC frames exposed to cyclic lateral loads. *Bulletin of Earthquake Engineering*, pp.1–26. Available at: <http://link.springer.com/10.1007/s10518-016-9929-0> [Accessed August 12, 2016].
- Polyakov, S.V., 1956. *Masonry in framed buildings (An investigation into the strength and stiffness of masonry infilling)*. Gosudarstvennoe izdatel'stvo Literaturny po stroitel'stvu i arkhitekture, Moscow. (English translation by G.L. Cairns, National Lending Library for Science.)
- Pryl, D. & Cervenka, J., 2013. *ATENA program documentation, part 1 of 1, troubleshooting manual*, Prague: Cervenka Consulting Ltd.
- Riddington, J.R. & Smith, B.S., 1977. Analysis of infilled frames subject to racking with design recommendations. *The Structural Engineer*, 55(6), pp.263–268.
- Saneinejad, A., 1990. *Non-linear analysis of infilled frames Part 1*. University of Sheffield.
- Saneinejad, A. & Hobbs, B., 1995. Inelastic design of infilled frames. *ASCE Journal of Structural Engineering*, 121(4), pp.634–650.
- Sarhosis, V., Tsavdaridis, K.D. & Giannopoulos, I., 2014. Discrete element modelling of masonry infilled steel frames with multiple window openings subjected to lateral load variations. *The Open Construction and Building Technology Journal*, 8(1), pp.93–103.
- Shimazaki, K. & Sozen, M.A., 1984. *Seismic drift of reinforced concrete structures*, Tokyo, Japan.
- Sigmund, V. & Penava, D., 2013. Assessment of masonry infilled reinforced concrete frames with openings. *Technical Gazette*, 20(3), pp.459–466.
- Sigmund, V. & Penava, D., 2014. Influence of openings, with and without confinement, on cyclic response of infilled R-C frames - An experimental study. *Journal of Earthquake Engineering*, 18(1), pp.113–146.
- Smith, B.S., 1966. Behaviour of square infilled frames. *Journal of the Structural Engineering Division, Proceedings of the American Society of Civil Engineers*, 92, pp.381–403.
- Sozen, M.A., 2014. Surrealism in facing the earthquake risk. *Geotechnical, Geological and Earthquake Engineering*, 26.
- Stavridis, A., 2009. *Analytical and experimental study of seismic performance of reinforced concrete frames infilled with masonry walls*. University of California, San Diego.
- Stavridis, A. & Shing, P.B., 2010. Finite-element modeling of nonlinear behavior of masonry-infilled RC frames. *ASCE Journal of Structural Engineering*, 136(3), pp.285–296.